Electronic Research Archive

http://www.aimspress.com/journal/era

ERA, 32(2): 1082–1125.
DOI: 10.3934/era.2024053
Received: 09 October 2023
Revised: 24 November 2023
Accepted: 22 December 2023
Published: 25 January 2024

Research article

Modeling the SARS-CoV-2 sublineages XBB and BQ.1 in Mexico, considering multiple vaccinations, booster dose, waning immunity and cross-immunity

Ugo Avila-Ponce de León[1,*], **Angel G. C. Pérez**[2] **and Eric Avila-Vales**[2]

[1] Human Systems Biology Laboratory, Instituto Nacional de Medicina Genómica (INMEGEN), Mexico City, Mexico

[2] Facultad de Matemáticas, Universidad Autónoma de Yucatán, Anillo Periférico Norte, Tablaje Catastral 13615, C.P. 97119, Mérida, Yucatán, Mexico

* **Correspondence:** Email: uapdl@hotmail.com.

Abstract: In a population with ongoing vaccinations, the trajectory of a pandemic is determined by how the virus spreads in the unvaccinated, vaccinated without boosters, and vaccinated with boosters, which will exhibit distinct transmission dynamics based on different levels of natural and vaccine-induced immunity. We found that enhancing the use of face masks in a partially vaccinated population is associated with a reduction of new infections, hospitalizations, and deaths. We highly recommend the use of a face mask with at least a 50% efficiency, such as improved cloth and surgical face masks, due to its effectivity and cost ratio. Our simulations indicated that there may be two upcoming Omicron waves (in the last months of 2022 and in May 2023). The magnitude of these waves will be 75% and 40% lower than their prior wave. Moreover, the size of these waves is heavily influenced by immunity parameters like waning immunity and cross-immunity protection. Hence, we recommend continuing the use of face masks to decrease transmission because we are not developing sterilizing immunity if we get infected by a prior sublineage, meaning that we can still get infected regardless of the acquired immunity.

Keywords: Omicron; vaccination; waning immunity; ordinary differential equations; Mexico; vaccine heterogeneity; COVID-19

1. Introduction

Since the beginning of the pandemic of COVID-19, at least 771 million confirmed cases and 6.97 million deaths have been reported (November 2023) [1]. In particular, Mexico has reported 7.6 million cases and a death toll of 334,752 [2]. In 2020, Mexico entered a social distancing period

called "Jornada de Sana Distancia" from March all the way through June 2020 as a non-pharmaceutical intervention that helped reduce the transmission of the virus [3]. Although social distancing requirements were relaxed by June 2020 through a system of traffic lights, the use of face masks in closed and open spaces was always "mandatory" [4]. Two years have passed and the use of face masks in Mexico is still being applied by the population. At the end of 2020, the "Comisión Federal para la protección contra riesgos sanitarios" (COFEPRIS) approved the use of a highly efficacious vaccine against COVID-19 (developed by Pfizer) [5], which was applied to our first line of defense, consisting of doctors and nurses. The strategy for vaccine application in Mexico was the same used by other countries, which focused on vaccinating the elderly to avoid more fatalities, as recommended by a series of mathematical models [6, 7]. The strategy was divided into six stages: vaccines would be first applied to workers associated with healthcare, then teachers, followed by adults divided by age: older adults, 50–59 years old, 40–49 years old, and the rest of the population [8]. Notwithstanding the similarity of Mexico's vaccination plan against COVID-19, the difference with other countries is the heterogeneity of vaccine brands being applied. Mexico has signed and applied 7 types of vaccine brands with three types of technology for the making of the vaccine. We have the mRNA vaccines Pfizer and Moderna; the non-replicating viral vector vaccines CanSino, Sputnik V, AstraZeneca, and Johnson & Johnson; and the inactivated vaccine Sinovac [5].

There have been some mathematical models that evaluated vaccination programs [9–12]. In [9], Alvarez et al. used a simple system of ordinary differential equations (ODEs) to assess the importance of a high vaccination rate instead of a high coverage in reducing the number of infected individuals. In [10], Munguía-López et al. focused on an optimization strategy to guarantee a fair allocation of the distribution of the vaccines to all states in Mexico under different fairness schemes. Soria-Arguello et al. [11] analyzed how to distribute the vaccine based on several transportation modes to guarantee a correct distribution to all the states in Mexico. Saldaña et al. [12] developed a mathematical model where they included the mobility of a population, vaccine coverage, efficacy, and delivery time. The study found that by reducing the mobility between patches, the burden of infections will diminish the same as with a 30% immunization in the population. They also showed that by increasing vaccine coverage between 20% and 50%, the reduction of infection can be up to 30% and 50%, respectively. However, none of these works have focused on the heterogeneity of vaccines in Mexico based on their efficiency, which is one of our main concerns in this study.

One year after the start of the pandemic (2021), the dynamics of the spread of the virus changed because of the implementation of the vaccines and the emergence of new variants which has not stopped since 2021. Based on their varied levels of infectiousness, lethality, and response to the vaccine, the most threatening ones are identified as variants of concern (VOCs) [13]. The first VOC that appeared was the Alpha variant (B.1.1.7 under the Pango lineage) that gained prevalence in the first half of 2021 [14]; nevertheless, this variant failed to become the dominant variant in Mexico because it could not compete with the Mexican variant that circulated until May 2021 [15, 16]. Instead, the Delta variant did not have the same behavior as Alpha, and it became the dominant variant in a short time until early December 2021 [17]. The Omicron variant was first detected in South Africa at the beginning of November 2021 [18, 19]. This variant was the cause of the rise in new cases at the beginning of 2022 in the whole world. The Delta variant became dominant in most countries within two weeks since it was first detected due to its high transmissibility and higher immune escape from the protection provided by the vaccine or natural infection [20]. Since the

variant emerged, around 5 sublineages have appeared, with BA.1 being responsible for the first wave of this variant. In the middle of 2022, the second wave of cases emerged with the sublineage BA.5 being responsible for this augmentation. This variant has mutations in the spike protein, developing a higher capacity of invading the host cell and evading the neutralizing function of antibodies [21, 22]. Moreover, people who got infected in the first wave can still get re-infected with this strain [23]. In Mexico, the Omicron sublineage XBB.12.1 was dominant in the first two weeks of June 2022, and recent data shows that BQ.1 is the current strain that predominates the new infections [24]. At the end of 2022, two new sublineages: XBB and BQ.1 emerged and competed between them to see who will become the dominant variant.

Two new variables need to be incorporated to understand the dynamics of subsequent waves of Omicron: the waning immunity (either acquired through the vaccine or natural) and the existence of boosters. In Mexico, the first reinforcement or booster began to be administered at the beginning of December 2021 and the application was completed until February 2022 [25], and the second booster started in May 2022 [8]. It is important to notice that a second booster is the fourth dose for all those whose first series consists of two doses (Pfizer, Moderna, Sputnik V, AstraZeneca, and Sinovac) and the third dose for those whose first series consists of only one dose (Cansino and Johnson & Johnson). The purpose of this study is to implement a mathematical model to understand the impact of the boosters on the dynamics of new cases, keeping in mind the waning of said booster in the remainder of this year. We will still incorporate the widespread use of face masks in the model because in Mexico this NPI is still being used to curtail infections.

Recently, some mathematical models have been proposed to explain the dynamics of the Omicron wave using a deterministic system of nonlinear differential equations [26–29]. In [26], Benahmadi et al. used a modified susceptible-infected-recovered (SIR) model to include vaccination and fitted the parameters with the dynamics of Omicron in Morocco. They developed an optimized control analysis based on an imperfect vaccine to diminish the burden of new COVID-19 cases. In [27], Edholm et al. used a modified SIR model that included vaccination and breakthrough (individuals who get infected despite being vaccinated) exposed individuals in the province of Gauteng, South Africa. Their main result is that modifying the rates of the two different vaccines has the ability to affect the spread of the virus. Meanwhile, Gonzalez Parra and Arenas [28] developed an SIR model to assess the importance of vaccination and how the waning immunity and the efficacy of the vaccine are important parameters that affect the spread of Omicron in the United States. Finally, Safdar et al. [29] developed an extensive modified SIR model to acknowledge the presence of three types of vaccines applied in the US and how they can prevent more new COVID-19 infections. In this model, the authors also included the notion of a booster (third dose for mRNA vaccines and second dose for Johnson & Johnson) and studied how a high percentage of the booster is needed to prevent more infections at the beginning of 2023. In the present work, we developed a mathematical model of the same characteristics that incorporates the perks of the vaccination program in Mexico and the current knowledge of the changing epidemiology of COVID-19 [30], including parameters that describe the waning of vaccine-derived and natural immunity, as well as the use of face masks with their different efficiencies and mixed cross-immunity between Omicron sublineages. To our knowledge, there are no current mathematical models that describe the dynamics of the second Omicron wave in Mexico and provide short-term predictions of that wave.

2. Materials and methods

In the following subsections, we describe the derivation of the mathematical formulas and parameter estimation for the model, including the parameters to explain the behavior of an imperfect vaccine. We also document the procedures for obtaining the control reproduction number, as well as the local sensitivity analysis.

2.1. Derivation of the mathematical model of a partially vaccinated population of Mexico, considering the application of multiple vaccines and waning immunity for two sublineages of Omicron

Our model was developed by modifying a previously developed compartmental mathematical model that incorporated vaccination in Mexico [31] mixed with a model that incorporated multiple vaccines as an important variable [32]. Because we are modeling a vaccination campaign against COVID-19, we must incorporate concepts around an imperfect vaccine into our model, such as leakiness and the all-or-nothing protection, which are well explained in [33, 34]. In view of the fact that the third Omicron wave in Mexico was first driven by the XBB and then by BQ.1, our mathematical model incorporates these two sublineages by adapting a previous compartmental model [35]. Finally, our model also incorporates the loss of immunity, either natural or acquired, and the existence of individuals with one or two boosters. The mathematical model contains two separate sets of equations for the Omicron variants XBB and BQ.1, which can affect the susceptible, vaccinated (regardless of the number of doses), and the partially protected susceptible individuals. Our compartmental models evaluate the dynamics of 16 populations at any given time t, which are denoted as $S(t)$, $F(t)$, etc. The flow between the compartments is represented in Figure 1.

Susceptible individuals will decrease when they interact with a symptomatic individual infected with BA.2 at a rate β_1 and with an asymptomatic individual at a rate β_2. Once exposed to the BA.2 sublineage, the infected individuals will become infectious after $1/w$ days. But only a proportion p_1 of these individuals will develop symptoms, whereas the rest of the exposed individuals will be asymptomatic. The symptomatic subpopulation can flow between two states: recovered or hospitalized. Symptomatic and asymptomatic individuals infected with BA.2 will recover after $1/\gamma_1$ days. However, in the case of symptomatic individuals, only a proportion $1 - \varphi_1$ recovers from the disease; the rest of them become hospitalized after $1/\sigma$ days, and these individuals can recover at a rate $\omega_1(1 - \chi_1)$ or die at a rate $\omega_1\chi_1$.

The second set of equations acknowledges the effects of individuals infected with BA.5, the flow between these compartments is the same as described for the BA.2. Partially protected susceptible individuals represent the compartment where immunity (either vaccine-acquired or naturally acquired) wanes and can be re-infected with the same or the other sublineage, it is depicted in Figure 1 as S_p. A full description of the model and the set of equations can be found in Appendix A1.

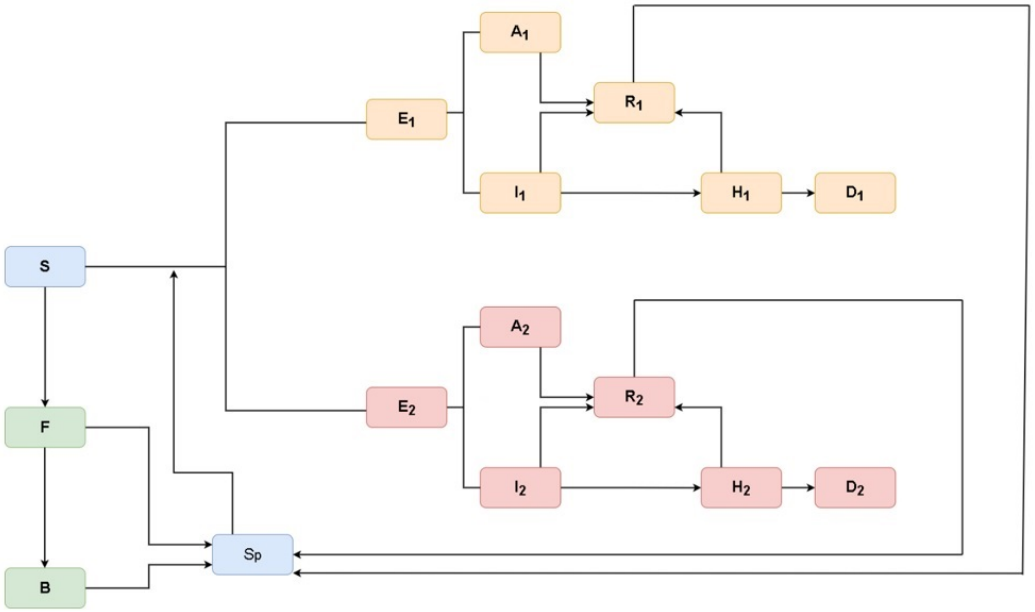

Figure 1. Schematic of the model considering multiple vaccines, waning immunity, and a partially protected population of two sublineages in Mexico. Flow dynamics of the mathematical model. S: unvaccinated susceptible, F: vaccinated with no booster doses, B: vaccinated with one or two boosters. E_1: exposed individuals with BA.2, I_1: infectious with BA.2 with symptoms, A_1: infectious with BA.2 without symptoms, H_1: hospitalized individuals with BA.2, R_1: recovered individuals from BA.2, and D_1: deceased individuals from BA.2. E_2: exposed individuals with BA.5, I_2: infectious with BA.5 with symptoms, A_2: infectious with BA.5 without symptoms, H_2: hospitalized individuals with BA.5 R2: recovered individuals from BA.5, and D_2: deceased individuals from BA.5. S_p: partially protected individuals whose immunity (acquired or natural) is decreasing.

2.2. Description of the parameters used as fixed values in the mathematical model of a partially vaccinated population of Mexico, considering the application of multiple vaccines and waning immunity for two sublineages of Omicron

To model the dynamics of the susceptible population, we use several parameters that need to be explained to better understand the dynamics of the spread of the two sublineages of Omicron. The first terms describe the dynamics of the population in question: Λ and μ describe the natural recruitment and the natural death rate, respectively. The following parameters need to be included in our model because we are not considering a closed population: individuals migrate to the population (Λ), and they may die due to causes other than COVID-19 (μ). Since we are considering two sublineages of Omicron, the susceptible population can be infected by both types of viruses; consequently, we have four transmission rates: β_1, β_2, β_3, and β_4. The first two parameters model the infection by sublineage one: β_1 represents when a susceptible individual encounters a symptomatic individual and β_2 represents when a susceptible individual interacts with an asymptomatic individual. Because asymptomatic people normally do not show symptoms, the probability of them infecting an individual is different than a symptomatic individual. Parameters β_3 and β_4 describe the same

dynamics as the latter, the only difference is that the susceptible individuals can get infected by the sublineage two when they interact with a symptomatic and an asymptomatic individual, respectively. Because we are modeling an imperfect vaccine, as explained in the previous section, all individuals that get vaccinated at a rate ρ may or may not be protected. We assume that only a proportion $\varepsilon_0 \in [0, 1]$ of the people receiving the vaccine are protected. This is called the "all-or-nothing" protection and is defined by the expression

$$\varepsilon_0 = \sum_{i=1}^{3}(1 - \varepsilon_{ai})w_i,$$

where ε_{ai} and w_i are the protection parameter and the relative vaccination rate, respectively, for each group of vaccines (high, medium, or low efficiency).

The next compartment consists of the fully vaccinated individuals, regardless of the manufacturer of the vaccine and the number of doses. Another concept related to vaccination is the vaccine effectiveness, which means that some individuals may get infected with either sublineage despite being vaccinated. This is what we will call "breakthrough infections". Because these individuals are vaccinated, they have developed a protection created by the vaccine, so if they encounter a symptomatic or asymptomatic individual infected with sublineage one, the probability of them getting infected is reduced by a rate $\mathcal{E}_1$. The same dynamic happens if they interact with an individual infected with sublineage two, the probability of infection is reduced by a rate $\mathcal{E}_2$. These parameters are defined as

$$\mathcal{E}_1 = \frac{1}{3}\sum_{i=1}^{3}(1 - \varepsilon_{1i}), \qquad \mathcal{E}_2 = \frac{1}{3}\sum_{i=1}^{3}(1 - \varepsilon_{2i}),$$

where ε_{1i} is the efficacy against sublineage one and ε_{2i} is the efficacy against sublineage two, for vaccines in the i-th group ($i = 1, 2, 3$). Some fully vaccinated individuals will stay for a period in this compartment because of the protection provided by the vaccine; however, the acquired immunity will wane against time, and they transit to a partially protected susceptible compartment at a rate α_B. In the fall of 2022, fully vaccinated individuals had the option of a booster dose, so this population may receive a booster at a rate ρ_B.

Booster individuals are the population that received an extra dose of vaccine to acquire more protection in the fall and winter of 2022; however, they can still get infected if they interact with infected individuals, regardless of their symptoms. Their probability of infection is reduced by a factor $1 - \varepsilon_{B1}$ for sublineage one and $1 - \varepsilon_{B2}$ for sublineage two. Eventually, the protection provided by the vaccine will wane over time, and these individuals will transit to a partially protected population at a rate α_B.

Exposed individuals, regardless of the sublineage, are those that are exposed to the virus because they encountered an individual infected with either sublineage of Omicron. The flow of this compartment comes from the susceptible population, breakthrough infections from fully vaccinated and booster dose, and from partially immune susceptible individuals. Partially immune protected individuals can get infected from sublineage one of Omicron at a rate reduced by a factor $1 - \psi_1$, and they can get infected by sublineage two at rate reduced by $1 - \psi_2$. As the immunity wanes, people can still get infected by the virus; however, they already have a targeted immune response that will prevent hospitalization.

A proportion of infected individuals will develop symptoms at a rate $p_1 w$ for sublineage one and $p_2 w$ for sublineage two. Most infected individuals will recover at a rate $\gamma_1 (1 - \varphi_1)$; however, a portion $\varphi_1 \in [0, 1]$ of these individuals will develop severe symptoms and can get hospitalized at a rate $\sigma\varphi_1$ for sublineage one. Meanwhile, for the sublineage two of Omicron, individuals will recover at a rate $\gamma_2 (1 - \varphi_2)$, and a portion $\varphi_2 \in [0, 1]$ of them may develop symptoms and will need to be hospitalized at a rate $\sigma\varphi_2$.

In the hospitalized compartment for both sublineages of Omicron, individuals will eventually recover and transit to the recovery compartment for sublineage one at a rate $1 - \chi_1$ multiplied by the average time of staying in hospital ω_1. Unfortunately, a proportion $\chi_1 \in [0, 1]$ of hospitalized individuals may pass away from the disease at a rate $\omega_1\chi_1$. Concurrently, hospitalized individuals from sublineage two will recover at a rate $1 - \chi_2$, multiplied by the average time in the hospital ω_2. In the same manner, a portion $\chi_2 \in [0, 1]$ of hospitalized individuals from sublineage two may die from the disease at a rate $\omega_2\chi_2$.

For recovered individuals from a previous infection by either sublineage of Omicron, their natural immunity would wane off at rates η_1 and η_2 for sublineages one and two of Omicron, respectively. All baseline parameters are outlined with their respective value and units in Table 1. Meanwhile, parameters associated with infection ($\beta_1, \beta_2, \beta_3, \beta_4$), hospitalization ($\chi_1$ and χ_2), recovery (φ_1 and φ_2), and vaccination rates (ρ and ρ_B) are estimated based on data. The description of the optimization protocol is mentioned in the next subsection.

Table 1. Baseline parameter values used for simulations.

Parameter	Value	Units
Λ	4794.52	people/day
μ	2.1123×10^{-5}	1/day
w	1/2	1/day
p_1	1/9	-
p_2	1/9	-
γ_1	1/5	1/day
γ_2	1/5	1/day
σ	1/2	1/day
ε_0	0.9995	-
α	0.2	1/day
α_B	0.05	1/day
η_1	1/300	1/day
ϵ_{B1}	0.90	-
ϵ_1	0.723	-
ψ_1	0.35	-
η_2	1/300	1/day
ϵ_{B2}	0.85	-
ϵ_2	0.723	-
ψ_2	0.30	-

2.3. Estimation of the parameters of the dynamics of the two most abundant Omicron sublineages in Mexico

In this section, we will estimate the parameter values for our model. First, we fit the model solutions to real data during the period from December 7, 2021 to April 20, 2022, which is when the first Omicron sublineage was dominant in Mexico. We assume that all reported infections during this period belong to this strain. Hence, the variables of our model corresponding to strain 2 will be set to zero. We set the fixed parameter values shown in Table 1. We estimate the values for β_1, β_2, φ_1, χ_1, ω_1, ρ, ρ_B, and the initial exposed population $E_1(0)$ by fitting our model to the daily COVID-19 infection, death and hospitalization data, as well as the cumulative numbers of vaccinations and booster doses. The optimization of parameters was performed in Matlab by minimizing the sum of squared errors (SSE), which was computed as follows. For a given vector of parameters $\mathbf{x}$, we obtain the numerical solutions of our model using the ode45 solver. Then, the sum of squared errors is given by

$$SSE(\mathbf{x}) = \sum_{i=1}^{n_1} \frac{\left(I_i^{mod} - I_i^{rep}\right)^2}{\max_j I_j^{rep}} + \sum_{i=1}^{n_2} \frac{\left(A_i^{mod} - A_i^{rep}\right)^2}{\max_j A_j^{rep}} + \sum_{i=1}^{n_3} \frac{\left(D_i^{mod} - D_i^{rep}\right)^2}{\max_j D_j^{rep}} + \sum_{i=1}^{n_4} \frac{\left(H_i^{mod} - H_i^{rep}\right)^2}{\max_j H_j^{rep}} + \sum_{i=1}^{n_5} \frac{\left(V_i^{mod} - V_i^{rep}\right)^2}{\max_j V_j^{rep}} + \sum_{i=1}^{n_6} \frac{\left(B_i^{mod} - B_i^{rep}\right)^2}{\max_j B_j^{rep}},$$

where I_i^{mod}, A_i^{mod}, D_i^{mod}, H_i^{mod}, V_i^{mod}, and B_i^{mod} are the number of new symptomatic infections, new asymptomatic infections, new deaths, active hospitalizations, cumulative vaccinations, and booster doses obtained from the model for the i-th day, respectively, while I_i^{rep}, A_i^{rep}, D_i^{rep}, H_i^{rep}, V_i^{rep}, and B_i^{rep} are the homologous quantities obtained from the reported data, respectively. Notice that the number of data points $n_1 \ldots, n_6$ may be different for each variable. During this period, the number of boosters was reported only for the final date (April 20, 2022), so we used this single value to compute the SSE by setting $n_6 = 1$. The parameter vector that minimizes the SSE was found using three searches: a gradient-based method, a gradient-free algorithm, and again, a gradient-based method.

The data for COVID-19 cases and deaths were obtained from [36]. The data for hospitalized cases were taken from [37], and the data for the number of vaccinations and booster doses were taken from [38]. The initial values for all variables other than E_1 were chosen according to these data. The best fit values are shown in Table 2. Figure 2 shows a comparison between the solutions obtained with the model and the reported number of symptomatic/asymptomatic cases, hospitalizations, and number of COVID-19 deaths. Figure 3 shows a similar comparison for the vaccinated population, and Figure 4 depicts the model solutions for the other variables.

Next, we estimate the values of β_3, β_4, φ_2, χ_2, ω_2, and ρ_B, using the model simulations for both strains for two different periods (April 20 to July 15, 2022 and November 18 to December 31, 2022). The other parameter values are fixed as before. The optimization for the first period was carried out using the same method as before but considering the cumulative numbers of COVID-19 cases and deaths, as well as the daily hospitalizations and booster doses. The initial conditions were chosen using the values obtained in the previous simulations for April 20, 2022.

The best fit parameters for the two-strain model are shown in Table 3. Figure 5 depicts a comparison between the model solutions and the reported number of symptomatic/asymptomatic cases, hospitalizations, and number of COVID-19 deaths (for both strains). Figure 6 shows a

comparison for the vaccinated population. Figure 7 depicts the model solutions for the susceptible, susceptible with variable immunity, and exposed populations. Figure 8 shows the simulated number of active infections and hospitalizations for each strain. These results were used to estimate the initial conditions for the optimization starting on November 18.

The comparison with reported data from November 18 to December 31, 2022 can be seen in Figure 9 (the number of vaccinations was not used in this case due to scarcity of reported data for this period), and simulations for both strains are depicted in Figure 10. The simulations show that the number of exposed, symptomatic, and asymptomatic individuals for strain 1 is almost zero for this period, while the number of hospitalized individuals is less than five for strain 1. This shows that strain 2 is dominating the pandemic dynamics from November 2022 onwards.

Table 2. Best fit parameters for strain 1 estimated from December 7, 2021 to April 20, 2022.

Parameter	Value	Units
β_1	1.3542×10^{-5}	1/day
β_2	0.3165	1/day
φ_1	0.02164	-
χ_1	0.3	-
ω_1	0.06346	1/day
ρ	0.003484	1/day
ρ_B	0.2322	1/day
$E_1(0)$	1.2457×10^6	people

Table 3. Best fit parameters estimated for strain 2 for the time periods April 20 to July 15, 2022 and November 18 to December 31, 2022.

Parameter	Value (Apr. 20–Jul. 15)	Value (Nov. 18–Dec. 31)	Units
β_3	6.4451×10^{-5}	8.3163	1/day
β_4	0.7335	2.9654×10^{-5}	1/day
φ_2	0.5	0.03543	-
χ_2	0.1247	0.2498	-
ω_2	8.8916×10^{-7}	0.02288	1/day
ρ_B	9.9932	9.9508	1/day

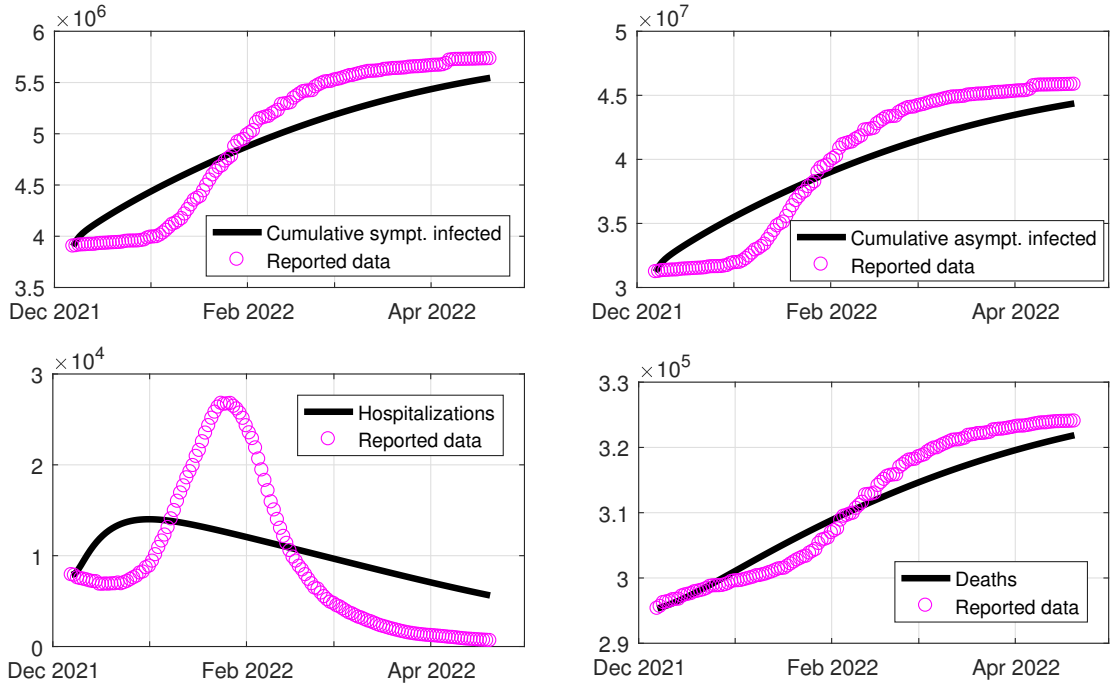

Figure 2. Comparison of reported data from December 7, 2021 to April 20, 2022 and simulations for the model with only one strain. Top left: cumulative number of symptomatic infected cases. Top right: cumulative number of asymptomatic infected cases. Bottom left: number of hospitalizations. Bottom right: death toll.

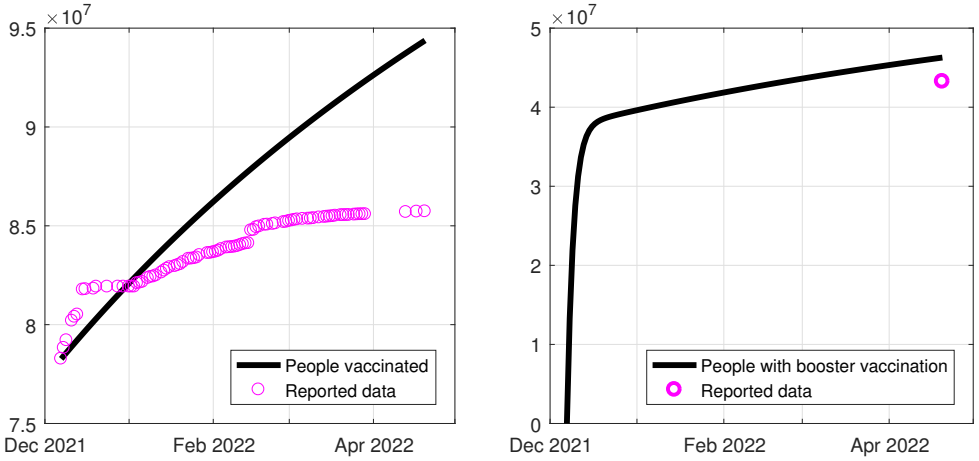

Figure 3. Comparison of reported data from December 7, 2021 to April 20, 2022 and simulations for the model with only one strain. Left: number of people vaccinated with at least one dose. Right: number of people with at least one booster vaccination dose.

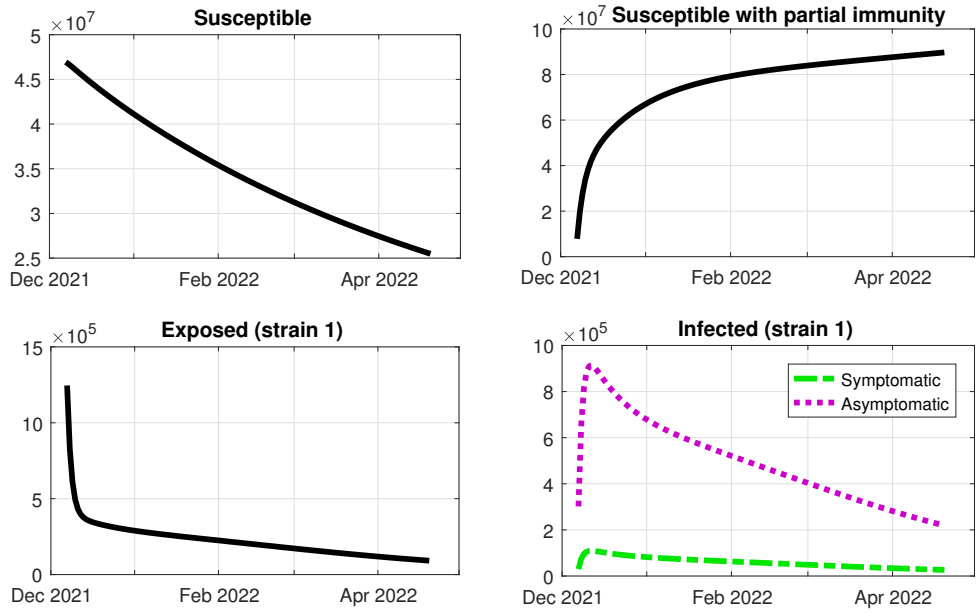

Figure 4. Simulations for the model with only one strain from December 7, 2021 to April 20, 2022. Top left: susceptible individuals. Top right: susceptible individuals with partial immunity. Bottom left: exposed individuals. Bottom right: active infected cases.

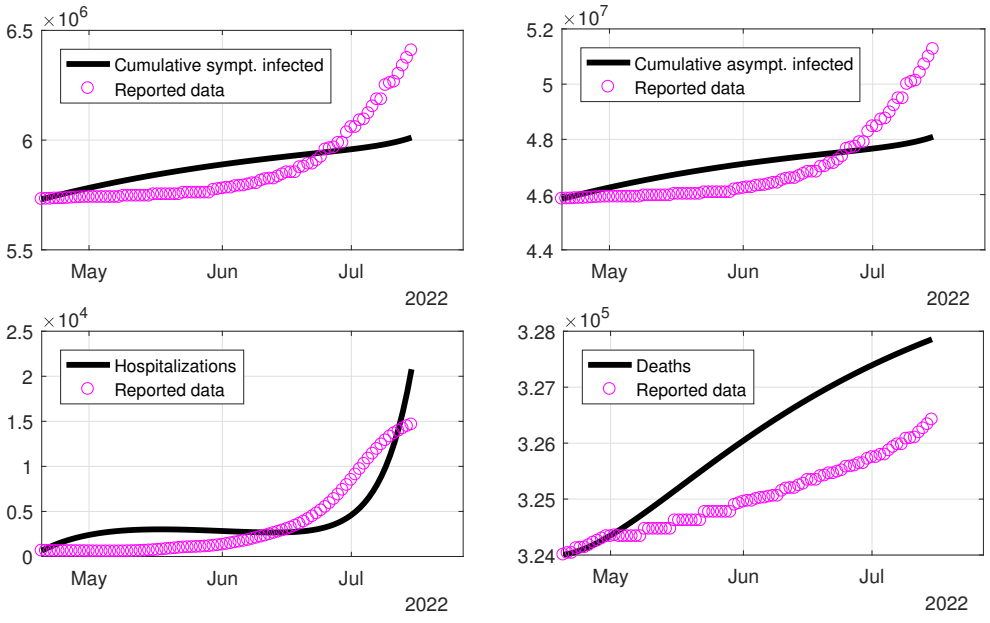

Figure 5. Comparison of reported data from April 20 to July 15, 2022 and simulations for the model with two strains. Top left: cumulative number of symptomatic infected cases. Top right: cumulative number of asymptomatic infected cases. Bottom left: number of hospitalizations. Bottom right: death toll.

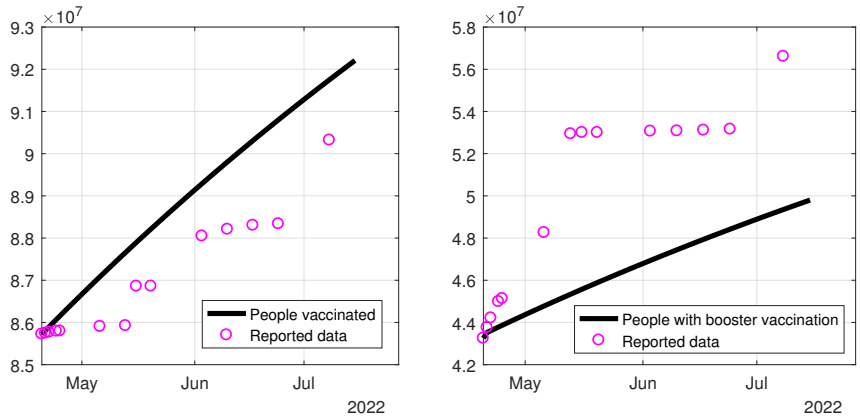

Figure 6. Comparison of reported data from April 20 to July 15, 2022 and simulations for the model with two strains. Left: number of people vaccinated with at least one dose. Right: number of people with at least one booster vaccination dose.

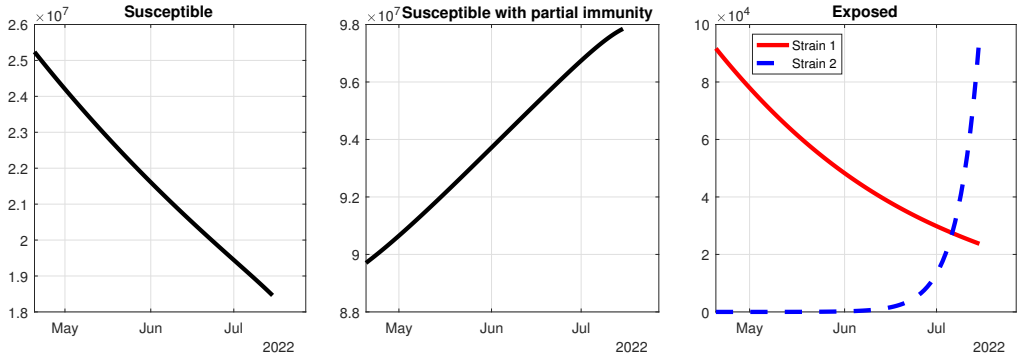

Figure 7. Simulations for the model with two strains from April 20 to July 15, 2022. Left: susceptible individuals. Center: susceptible individuals with partial immunity. Right: exposed individuals.

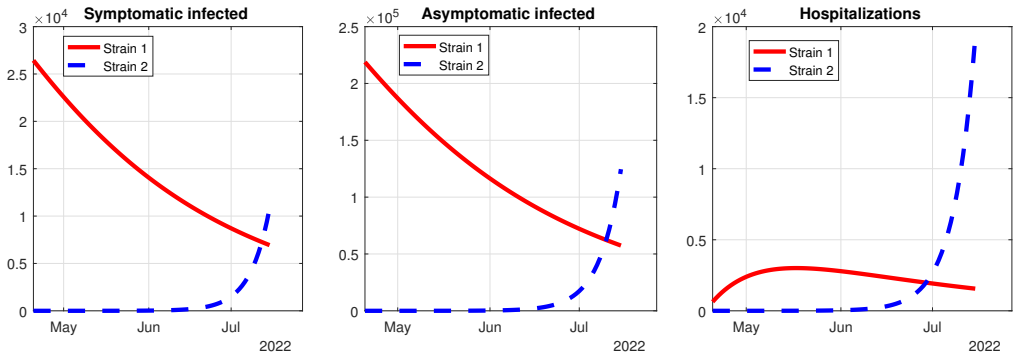

Figure 8. Simulations for the model with two strains from April 20 to July 15, 2022. Left: active symptomatic infected cases. Center: active asymptomatic infected cases. Right: hospitalizations.

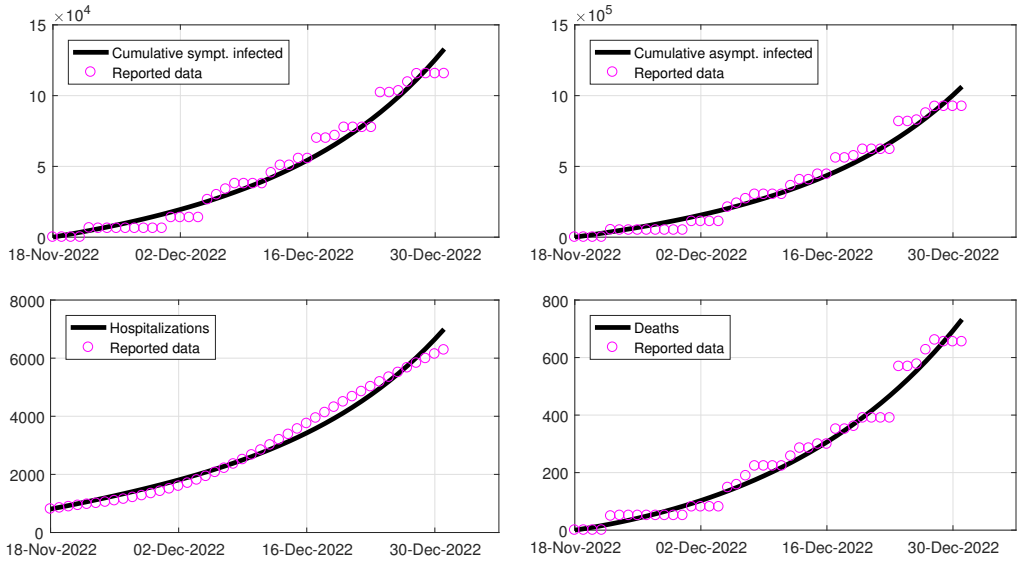

Figure 9. Comparison of reported data from November 18 to December 31, 2022 and simulations for the model with two strains. Top left: cumulative number of symptomatic infected cases. Top right: cumulative number of asymptomatic infected cases. Bottom left: number of hospitalizations. Bottom right: death toll.

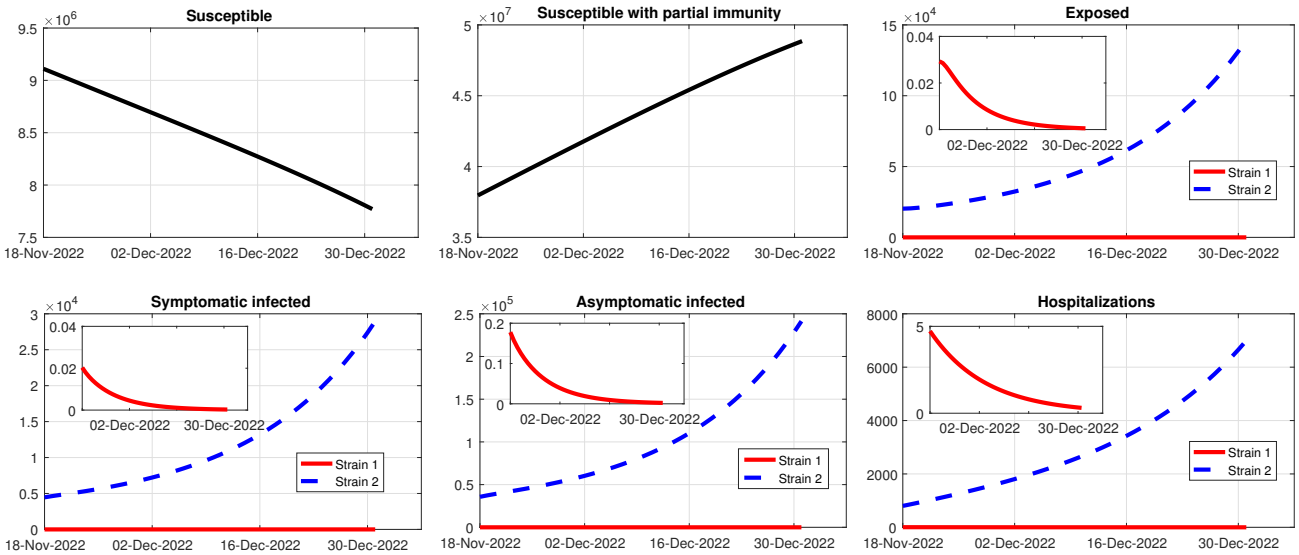

Figure 10. Simulations for the model with two strains from November 18 to December 31, 2022. Top left: susceptible individuals. Top center: susceptible individuals with partial immunity. Top right: exposed individuals. Bottom left: active symptomatic infected cases. Bottom center: active asymptomatic infected cases. Bottom right: hospitalizations. Insets show the corresponding curves for strain 1.

2.4. Estimation of the control reproduction number

Our model always has a disease-free equilibrium, which is given by

$$E_0 = (S^0, F^0, B^0, 0, 0, 0, 0, 0, S_p^0, 0, 0, 0, 0, 0),$$

where $S^0 > 0$, $F^0 \geq 0$, $B^0 \geq 0$, $S_p^0 \geq 0$ (the equalities hold in the case when there is no vaccination) and $E_1 = I_1 = A_1 = H_1 = E_2 = I_2 = A_2 = H_2 = 0$.

This equilibrium represents the scenario when the disease has become extinct, resulting in fixed fractions of the vaccinated, susceptible, and partially protected susceptible individuals. If the vaccination rate is positive, there will always remain a vaccinated portion and a partially protected portion of the population. Otherwise, if the vaccination program is discontinued, the entire population will become completely susceptible due to the waning rate of immunity.

We compute the control reproduction number $\mathcal{R}_c$ by applying the next-generation matrix method (see [39]) and using the equation $\mathcal{R}_c = \rho\left(FV^{-1}\right)$, where F denotes the derivative of the matrix of new infections, V is the transition matrix (flow between compartments), and ρ is the spectral radius. The entire derivation of the reproduction number, as well as the theoretical analysis of the model can be found in Appendix A2.

2.5. Local sensitivity analysis of the control reproduction number

The sensitivity analysis of the control reproduction number was carried out using the following definition, taken from [40]: the normalized forward sensitivity index of $\mathcal{R}_c$, which depends differentiably on a parameter p, is defined by

$$\Gamma_p^{\mathcal{R}_c} = \frac{\partial \mathcal{R}_c}{\partial p} \times \frac{p}{\mathcal{R}_c}.$$

Using the estimated values for the parameters obtained in Section 2.3 as baseline values, we were interested in perturbing them to determine how their changes affect the reproduction number $\mathcal{R}_c$. We used the software Maple to compute the partial derivatives of the reproduction number with respect to each parameter and then evaluate the sensitivity index, following the formula above. A positive sign of this index correlates with an increase in $\mathcal{R}_c$, whereas a negative sign is associated with a decrease in $\mathcal{R}_c$.

3. Results

3.1. Modeling the SARS-CoV-2 Omicron sublineages variant spread in a multiple vaccinated population

In this section, we simulated our model to evaluate the behavior of the usage of face masks, vaccination and the importance of the booster and waning immunity in Mexico. We considered seven types of vaccines that are currently being applied in Mexico: Pfizer, Moderna, Sputnik V, AstraZeneca, Johnson & Johnson, Cansino, and Sinovac. To simplify our model, we grouped the seven types of vaccines into three groups based on their efficiency in preventing symptoms when a person gets infected with the virus. Pfizer, Moderna, and Sputnik V are grouped as *high efficiency*; AstraZeneca and Johnson & Johnson are considered *medium efficiency*, and finally, Cansino and

Sinovac [41] consitute the *low efficiency* group. The simulations were carried out based on the estimated and fixed parameters presented in Tables 1–3.

Cases of infected individuals of the third wave of Omicron are starting to decrease, the peak was reached in the first week of January 2023 (Figure 11A). In the following months, cases of symptomatic individuals will start to descend, reaching a valley in the month of February for the XBB variant. In the last months of 2022 and early days of 2023, there will be a slight increase in cases, the peak may be reached in mid-March. Nevertheless, the peak will be 10 times higher than the peak reached between December and January 2023 with the XBB variant. The pattern of asymptomatic infections is the same as for symptomatic infections, the only difference is the number of cases. The peak was reached with less than 80,000 cases in the first week of January 2023, followed by a descent reaching a valley of zero active asymptomatic cases for the XBB variant, trailed to a peak in mid-December. The peak in the last month of the year will be 10 times lower compared with the peak that will be reached in March 2023 (Figure 11B). Notwithstanding an increase in cases, the number of hospitalizations will increase equally, but it will not be such a sudden increase that it exceeds the carrying capacity of medical supplies (Figure 11C). The peak was reached in the last week of December 2022 with a value of fewer than 2500 hospitalizations, the dynamics of descent will be the same as the infections and the peak of hospitalization may be until March of 2023 with roughly 250,000 hospitalizations, which will be more than 50% compared with the peak attained in the last week of the year (Figure 11C). Around 62% percent of the population of Mexico is fully vaccinated, and the trend of accomplishing the percentage to reach a higher population of vaccinated individuals is descending, which means that unvaccinated individuals will not be getting their dose of vaccine. Booster doses will continue to be applied in December with a descent in March 2023 (Figure 11D).

Now, we will review the behavior of the recovered, susceptible but partially protected individuals and the death toll by COVID-19. The recovery of individuals from XBB will continue to descend throughout the year, highlighting that it will never attain a value of zero-infected cases from this sublineage. In the meantime, the pattern of infections from BQ.1 will be decreasing for roughly two weeks and increasing in the following months, meaning that provided another variant or sublineage does not enter or emerge due to high transmission, BQ.1 will be circulating in the country going up and down in new infections (Figure 12A). In Figure 12B, we can acknowledge that the increase of new cases in the following months is caused by the dynamics of the susceptible but partially protected individuals, and that when this population decreases it will eventually be implicated in an increase of symptomatic or asymptomatic cases in the weeks following the decrease. When a period passes, the people who were not infected in the last wave of the year are the ones who will supply the next wave between the first months of 2023. The pattern of new infections will be dictated by this population, which derives from the fact that very few individuals will remain in the susceptible compartment without protection (Figure 12B). Because the cases of XBB are decreasing, the death toll from this sublineage will be zero; however, the pattern for BQ.1 is different (Figure 12C). By January 2023, there will be around 70,000 deaths because of their infection from BQ.1. If no other variant emerges in the remainder of the year, the death toll by BQ.1 sublineage may reach around 150,000 deaths in July 2023 (Figure 12C). This means that although the death rate is low, it will never be zero. Strategies must continue to be used to reduce transmission.

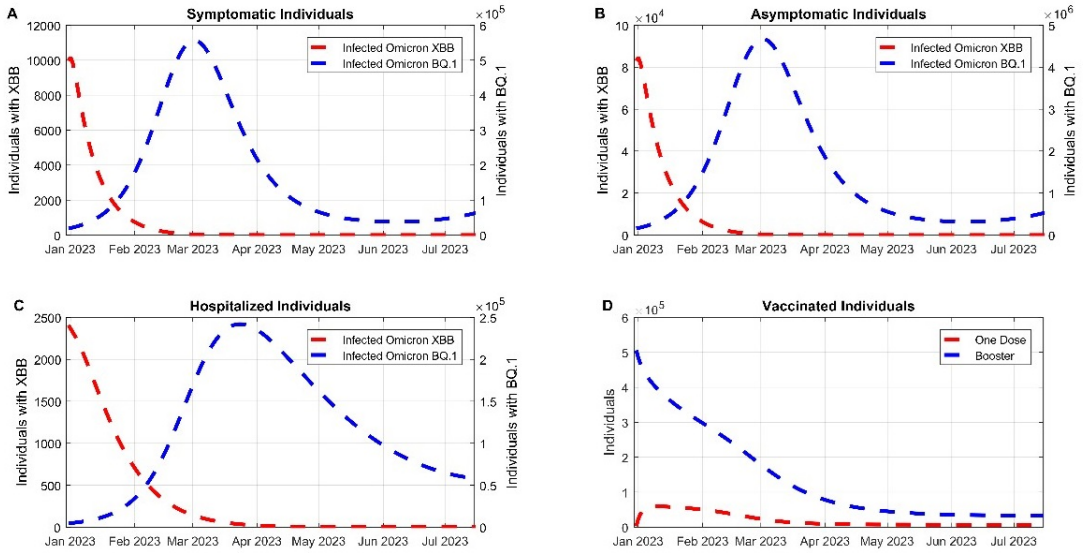

Figure 11. Simulation of the XBB and BQ.1 Omicron wave in Mexico, where 50% of the population wears a face mask. A: Symptomatic infected individuals of the Omicron variant; B: Asymptomatic infected individuals of the Omicron variant; C: Hospitalization dynamics of the Omicron variant; D: Vaccination status of the community of Mexico, based on the number of doses. Red denotes XBB, and blue denotes the BQ.1 sublineage.

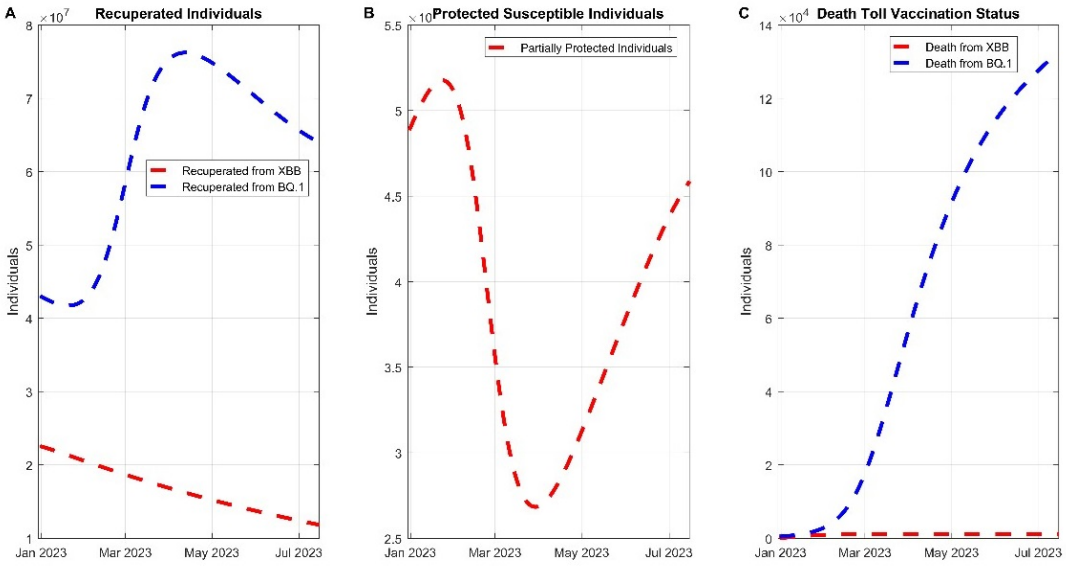

Figure 12. Simulation of the XBB and BQ.1 Omicron wave in Mexico, where 50% of the population wears a face mask. A: Recuperation of individuals; B: Partially protected susceptible individuals; C: death toll of the Omicron wave. Red denotes XBB, and blue denotes BQ.1.

3.2. *Spread of the Omicron variant under heterogeneity of vaccination efficiency due to the application of multiple vaccines*

Vaccines against COVID-19 have become the best strategy to decrease hospitalizations and deaths caused by this virus [42], and Mexico is not the exception. Less than 40% of the population in Mexico has not received a vaccine, which is still a significant amount, however, the population of susceptible but partially protected individuals is increasing because of the waning of natural or acquired immunity. The exposure rate of partially protected individuals is higher compared with the unvaccinated individuals (Figure S1), however, the probability to enter a hospital is greater in the unvaccinated population than in the partially protected population, regardless of the sublineage of Omicron (Figures 13 and S2). We separated the vaccinated population into two groups, those who received a booster and those who did not. The booster population has a higher exposure rate to the BQ.1 sublineage; however, their hospitalization rate is lower compared with the population that has not received any type of booster (Figure S3).

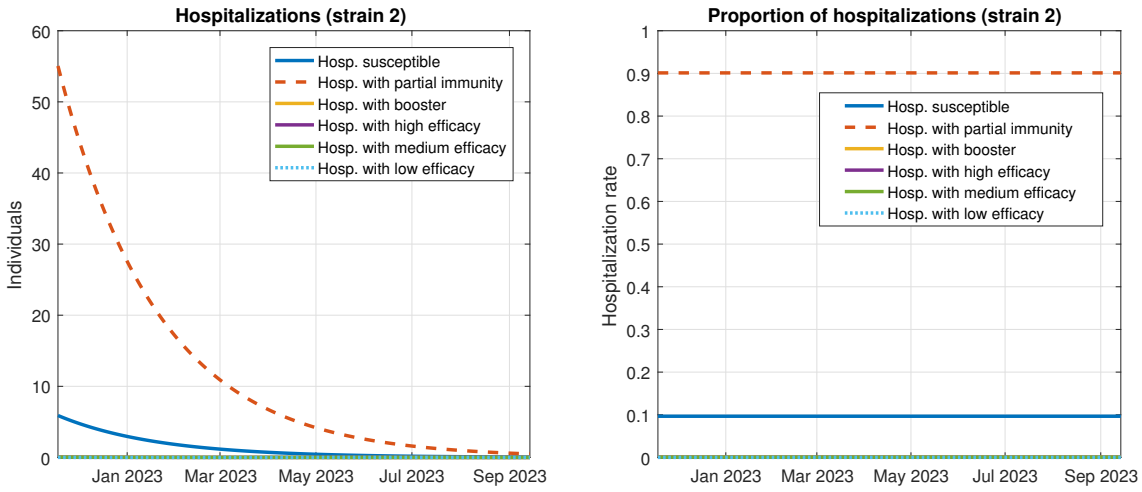

Figure 13. Hospitalizations for strain 2 (Omicron BQ.1) based on vaccination status. Left panel shows the number of hospitalized individuals in each subpopulation, right panel shows the proportion of each subpopulation with respect to the total hospitalizations for strain 2. The orange, purple, green, and light blue curves overlap, since they are very close to zero.

Finally, we wanted to evaluate how efficiently the three groups of vaccines that have been applied in Mexico have behaved in this second Omicron wave. The high-efficiency group had a lower exposed rate compared with the other efficiency groups, followed by the medium-efficiency group with a lower exposed rate compared with the low-efficiency group of vaccines applied in Mexico. This means that if a person is vaccinated with a low-efficiency vaccine, the probability of becoming exposed to the virus is higher than with other vaccines. Notwithstanding, this higher rate is not observed in the hospitalization rate: regardless of the vaccine, the proportion of hospitalization is relatively the same for the three groups of vaccines (Figures S2 and 13). For both sublineages, the hospitalization rate was higher for the susceptible non-protected individuals (Figures 13 and S2). Despite the heterogeneity of vaccines applied in Mexico, they have helped reduce the hospitalization rate, regardless of their vaccine

efficiency. One flaw observed in the vaccines against COVID-19 is that they reduce the transmission between individuals, although not significantly.

3.3. Assessing the impact of different combinations of COVID-19 vaccines

In this section, we will evaluate the combinations of vaccine efficiencies that can influence the infectivity of SARS-CoV-2 in Mexico. The vaccine with the highest number of doses applied in Mexico is AstraZeneca, followed by Pfizer [43]. Considering the three groups of vaccines applied in Mexico mixed with six combinations, we simulated the roll-out of new infections and hospitalization in this second Omicron wave. In Table 4, we list the combinations of the vaccines compared with the real strategy with their weighted average efficiency based on the administered doses. The first combination is the strategy applied by Mexico.

Table 4. Mixed vaccine proportions and combinations with their resulting specific efficiency. These values were used to simulate Figures S4 and S5.

High efficiency	Medium efficiency	Low efficiency	Resulting efficiency
34.4%	50.4%	15.2%	33%
100%	0%	0%	41%
0%	100%	0%	31%
0%	0%	100%	22%
33%	33%	33%	31%
30%	30%	40%	30%
50%	25%	25%	34%

We evaluated the peak that occurred in July–August 2022 and the peak that may occur between November and December 2022. We evaluated whether the original vaccination strategy had been modified from the beginning based on the combinations proposed in Table 4. First, we evaluated the differences with the peak of the second wave in 2022. If Mexico had decided to vaccinate with only high efficacy, in general, there would be a decrease of 0.0259%, 0.03%, 0.0308%, and 0.0024% of symptomatic and asymptomatic cases, hospitalizations, and deaths, respectively (Figure S4). In contrast, using only a medium efficacy vaccine, there would be a slight increase of 0.0103% and 0.005% of symptomatic and asymptomatic cases, respectively. With a slight increase in hospitalizations, at 0.006%, deaths from COVID-19 would have remained the same. Vaccination with only low efficiency will produce an increase of roughly 0.5792% symptomatic and 0.0303% asymptomatic infections. In the case of hospitalizations, there will be an increase of 0.0352%, and deaths from COVID-19 will be associated with a 0.0024% increase for the second peak of the Omicron wave. For the other comparisons, there will be a slight increase in cases if they present no symptoms, as well as in hospitalizations (Figure S5). Only when we vaccinate more with a low-efficiency vaccine will there be an increase of 0.0012% in the death toll in mid-July. The peaks for each vaccine strategy are shown in Table 5.

Table 5. Vaccine efficiency of the comparison with the current scenario for the peak in mid-July of cases (symptomatic or not), hospitalization, and deaths (Figure S6).

Vaccine strategy	Symptomatic	Asymptomatic	Hospitalizations	Deaths
Original	1.9338×10^6	1.9807×10^7	4.5465×10^5	8.4762×10^4
High efficiency only	1.9336×10^6	1.9801×10^7	4.5465×10^5	8.4760×10^4
Medium efficiency only	1.9340×10^6	1.9808×10^7	4.5468×10^5	8.4762×10^4
Low efficiency only	1.9345×10^6	1.9813×10^7	4.5481×10^5	8.4764×10^4
All the same	1.9340×10^6	1.9808×10^7	4.5468×10^5	8.4762×10^4
More low-efficiency	1.9340×10^6	1.9808×10^7	4.5469×10^5	8.4763×10^4
More high-efficiency	1.9338×10^6	1.9807×10^7	4.5463×10^5	8.4762×10^4

Now, we will evaluate the behavior for the third Omicron wave in the last months of 2022. Overall, the behavior in terms of decay maintains the same pattern as the peak of mid-July. In relation to symptomatic cases, there will be a decay independently of the application of high, medium, or low-efficiency vaccines only and the decay will be 0.0119%, 0.0158%, and 0.0222% respectively. For hospitalizations, there will be a decay only when we apply high-efficiency vaccines, for medium and low efficiency there will be an increase of 0.004% and 0.0168%, respectively. Deaths from COVID-19 will remain the same using only a high-efficiency vaccine, while for medium and low efficiency there will be an increase of 0.0054%. Using all combinations is associated with an increase or decrease; however, the change of values is slight and we do not consider it significant. The peaks for each vaccine strategy are shown in Table 6.

Table 6. Vaccine efficiency of the comparison with the current scenario for the peak in mid-November of cases (symptomatic or not), hospitalization, and deaths (Figure S7).

Vaccine strategy	Symptomatic	Asymptomatic	Hospitalizations	Deaths
Original	5.0610×10^5	5.3782×10^6	1.1911×10^4	1.8414×10^5
High efficiency only	5.0604×10^5	5.3777×10^6	1.1910×10^4	1.8414×10^5
Medium efficiency only	5.0612×10^5	5.3783×10^6	1.1912×10^4	1.8415×10^5
Low efficiency only	5.0618×10^5	5.3789×10^6	1.1913×10^4	1.841×10^5
All the same	5.0612×10^5	5.3783×10^6	1.1912×10^4	1.8415×10^5
More low-efficiency	5.0612×10^5	5.3784×10^6	1.1912×10^4	1.8415×10^5
More high-efficiency	5.0610×10^5	5.3781×10^6	1.1911×10^4	1.8414×10^5

3.4. Evaluating the vaccine efficiency for the primary application and boosters in the rollout of infections, hospitalizations, and death from COVID-19

We evaluated the importance of different vaccine efficiencies for the primary set of doses and the booster, as well as how both sublineages compete based on the overall efficiency provided by the vaccine. For individuals who have not received a booster, there is a significant difference in the number of symptomatic individuals when we compare the low and high efficiency of the vaccines. If the vaccine has the highest efficiency, there will be a reduction of roughly 0.0013% of cases compared with the baseline efficiency. When we compare with low efficiency, there could be an increase of

roughly 0.0016% in symptomatic infections (Figure 14A). The same pattern of increase and decrease occurs with the asymptomatic cases, hospitalizations, and death toll (Figure 14B–D). In terms of the competition between sublineages, vaccine efficiency helps in decelerating the increase of XBB infections, and this reduction was associated with an increase of BQ.1 infection. This means that XBB was the force for the third wave of Omicron in the last month of 2022 (Figure S6).

Booster doses behave in the same manner, that is, when the efficiency is high compared with the baseline, there will be a decrease in symptomatic cases (Figure S7A), asymptomatic cases (Figure S7B), hospitalizations, and deaths (Figure S7C,D). The opposite behavior occurs when we compare low efficiency with baseline efficiency. In terms of the competition between XBB and BQ.1, the same behavior occurs, XBB was the force to let BQ.1 thrive when the transmission was high. However, booster doses can reduce the peak that may occur in the first months of 2023 (Figure S8). This means that booster doses are more helpful in reducing the number of infected and hospitalized cases from the BQQ.1 Omicron variant.

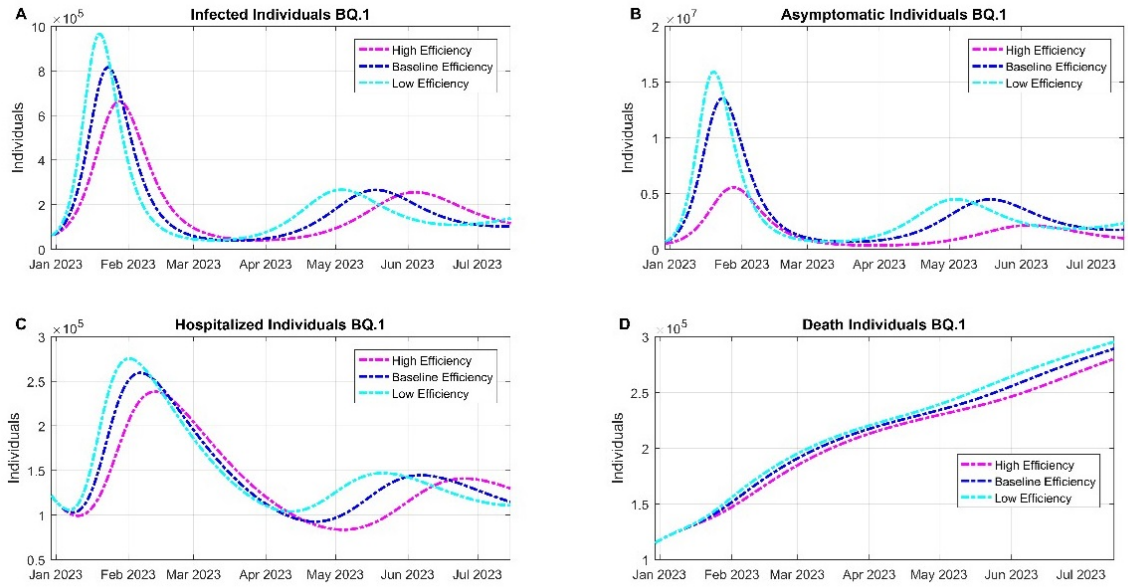

Figure 14. Vaccine efficiency in the primary application and boosters in Mexico. Dynamics for A: infected individuals, B: asymptomatic individuals, C: hospitalized, D: death individuals from the BQ.1 Omicron variant.

3.5. Assessing the importance of the use of a non-pharmaceutical strategy: face mask usage and efficiency are associated with shaping the behavior of the Omicron third wave

In this section, we evaluate the behavior of two important parameters: the proportion of the population that uses face masks ($C_m \in [0, 1]$) and the efficiency of the face masks ($\epsilon_m \in [0, 1]$) being used by said population. In Mexico, the use of face masks was not compulsory throughout the pandemic; however, most of the population used them and continue to wear them, specifically in closed areas. We evaluated four types of face masks: cloth masks, improved cloth masks, surgical face masks, and N95 face masks.

Cloth face masks have a 30% of protection against getting infected with the Omicron variant. In Figure S9, we evaluated three scenarios of the usage of cloth face masks based on the percentage of the population: from 25% to 75% of the population using face masks. If only 25% of the population uses a cloth face mask, the peak in March would have been roughly 466,130 symptomatic cases. In the meantime, if 50% of the population wears this type of face mask, there would have been a reduction of 18.74%, or roughly 87,340 fewer infected cases. Despite having a low efficiency in protection, the peak could have been reduced to only 298,570 active symptomatic cases if 75% of the population uses this face mask, a reduction of 35.95% of infected cases when compared with a 25% use of face masks. For the third wave in the last two months of the year, the difference in the percentage of use will dictate the time it takes to reach the peak. All three percentages will reach the same number of active symptomatic cases, and the difference is the length it takes to reach the peak. For asymptomatic individuals, if 75% of the population use face masks, the peak in March could have a 35.93% reduction and it will take roughly two months to achieve the peak in mid-April of 2023 (Figure S9B). Hospitalization is reduced in the same manner if only 50% of the population uses a face mask with low efficiency with a decrease of less than 14.16% admissions (Figure S9C). Deaths can be reduced by the beginning of 2023, with a minimum reduction of 15,401 deaths (28%) if 50% use this type face mask (Figure S9D).

If we reinforce our cloth face mask and add a tri-layer, which improves the efficiency to 50% of protection against the Omicron variant, the reduction is much more drastic. When 50% of the population uses it, the peak can be not only reduced but the time to reach the peak will be longer compared with a 25% use of this face mask. The symptomatic infections will be reduced with roughly 36.51% if only 50% of the population uses this face mask, compared with only 25% of usage. If 75% of the population uses the face mask, symptomatic active cases can be reduced by 363,575 infections, which is associated with a reduction of almost 90% compared with only 25% of usage (Figure S10A). The same pattern of reduction is observed in asymptomatic individuals (Figure S10B). Hospitalizations can be reduced by 99,495 (−49.56%) or 180,743 (−90.02%) if 50% or 75% of the population use this type of face mask, respectively, and the subsequent wave that may happen in the remaining of this year may be significantly reduced only if 50% or more people use this type of face mask (Figure S10C). The death toll is reduced if a minimum of 50% of the population uses this type of face mask (Figure S10D).

The most efficient face masks are the surgical and the N95, with 70% and 95% efficiency, respectively. However, the use of surgical face masks is slightly more accessible due to their cost compared with the N95. With only 25% of the population using this type of face mask, there would have been a significant amount of reduction than if no one uses it (Figure 15). By increasing to 50% the use of face masks, a considerable reduction of roughly 280,974 (−89.99%) infections, which is a significant reduction of cases when the transmission is high (Figure 15A). For the upcoming wave of 2023, the peak with 50% of usage is lower than when 25% of the population uses a face mask, a reduction of 10,000 active symptomatic cases. If we compare the 75% use of this face mask, two important effects are seen: the peak is reduced and the time it takes to reach the peak is larger. The peak will be reduced by 331,722 (−94.44%) active cases and it will be reached in roughly three months, enough time to reduce transmission and help gather medical supplies if needed. This pattern is observed in asymptomatic individuals with a reduction of the peak and 5 months to reach it (Figure 15B). For hospitalizations, the reduction is slightly more drastic. If 75% of the population

uses a surgical mask, there will be 163,360 (−95.94%) fewer hospitalized individuals in the peak for June 2023. In terms of the use of beds, this reduction is important to deal with other diseases that have been ignored because of this pandemic (Figure 15C). Deaths are more significantly reduced, with a decrease of roughly 30,477 deaths if 75% of the population uses a surgical mask and a decrease of 25,302 if 50% of the population uses it, compared with 25% of the population (Figure 15D).

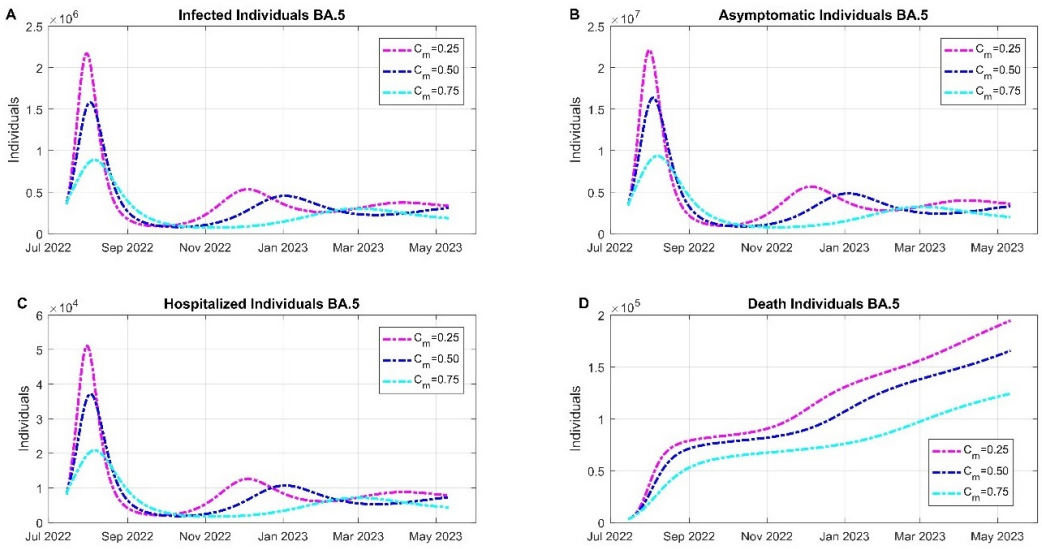

Figure 15. Evaluating the importance of the usage of face masks with a surgical face mask with 70% efficiency for the unvaccinated or vaccinated population. A: dynamics of the infected symptomatic individuals; B: asymptomatic infected individuals; C: variation of hospital admission; D: death toll of COVID-19. In all graphs, the pink dotted line represents that 25% uses face mask, and the blue dotted line denotes that 50% uses face masks. Finally, the cyan dotted line indicates that 75% of the population wears a face mask.

Next, we will evaluate the use of the N95 face masks, but we consider that, due to their cost, a large part of the population does not use this type of face mask. However, the reduction of new infections is drastic. If 50% of the population of the population uses an N95 mask, the peak of mid-April could have been reduced to only 19,588 symptomatic cases, and if 75% of the population uses it, the peak would have been reduced by 274,470 infected symptomatic cases compared with 50% of usage (Figure S11A). With a 25% usage, the peak in the last month of the year will be only 280,460 cases; however, it would take only one month to reach this peak. Nevertheless, if 50% uses this type of face mask, the peak can be reduced by 150,000 infected cases, and it will take roughly two months to reach it, which is a considerable time to prepare for the subsequent wave in terms of gathering medical supplies. On the other hand, if 75% of the population uses this face mask, the subsequent waves can be avoided and new infections will approach a value close to zero, a value not seen since the pandemic began (Figure S11A). The same dynamics occur with asymptomatic cases: if more individuals use this type of face mask, the subsequent waves will smaller compared to the last one, and the time it takes to reach them will be longer (Figure S11B). Hospitalizations are reduced by 105,930

individuals if 50% use an N95, compared with a reduction of 107,430 hospitalized individuals if 75% of the population uses it (Figure S11C). Deaths are significantly reduced: if 75% of the population uses an N95, there will be no more deaths caused by COVID-19 since September, however, there is an important reduction if only 50% of the population uses this type of face mask, deriving in 17,748 fewer deaths compared with 25% of the population using this type of face mask. In conclusion, face masks are an important non-pharmaceutical strategy that still needs to be implemented to reduce transmission and the probability of the emergence of new more infectious variants.

3.6. Varying the loss of acquired or natural immunity in a population that is continuously using face masks

In this section, we will evaluate how the loss of immunity once people get infected, regardless of vaccination status, will shape the behavior of the last wave in 2023. To better visualize the effect of this parameter, we divided the graphs into two periods, the wave in March (January–March 2023) and the wave that may happen in June (May–July 2023). If individuals recovering from COVID-19 developed lifelong protection by December 2022, the pandemic will not become extinct in that period: the number of infected symptomatic cases will be low, with only 296,110 cases (Figure S12, pink dotted line). However, as individuals can get re-infected from this virus, we varied the average immunity period between 50 days (red dotted line) and 150 days (black dotted line) with a baseline protection of 100 days (blue dotted line). The simulation was carried out assuming that a minimum of 50% of the population wears a face mask in the period evaluated, with an overall efficiency of 50% (improved cloth face mask). The dynamics of symptomatic and asymptomatic cases are highly influenced by the value of this parameter: if protection lasted only 50 days, this could result in a higher peak in February, with slightly more than 1,684,700 individuals with symptoms and 14,104,000 asymptomatic individuals (Figure S12A,B). The difference between the duration of 100 and 150 days is roughly 247,670 (−22.97%) symptomatic and a 2,068,900 (−2.29%) asymptomatic individuals (Figure S12A,B). The decay (at the end of March) followed by the peak in February has interesting dynamics for symptomatic, asymptomatic, and hospitalized individuals. A loss of protection in 50 days is results in a steady decay at the end of March 2023 with 468,870 symptomatic cases, 3,878,300 asymptomatic cases, and only 64,477 hospitalized individuals (Figure S12A–C). Instead, a loss of protection between 100 and 150 days will result in fewer than 279,410 active symptomatic cases at the end of March, 2,317,900 asymptomatic cases, and 47,165 hospitalized individuals (Figure S12A–C). Regardless of the duration of protection, all scenarios are associated with a stabilized behavior of infections at the end of March 2023. The death toll is affected by the re-infection parameter, where a 50-day period of protection yields a higher count with roughly 4458 more deaths compared with protection between 100 and 150 days (Figure S12D).

Now, we will assess the dynamics of cases between May and July 2023, the period where there may be a subsequent wave of Omicron. There is a difference of around two weeks in the time when the peak is reached when varying the loss of immunity: for 50 days, it will be reached in the second week of June; for 100 days, in the first two weeks of July 2023, and for 150 days, in the first two weeks of August 2023 (Figure 16). For a 50-day duration, symptomatic cases will peak at 985,000 and approximately 8,000,000 for asymptomatic cases (Figure 16A,B), and by the end of September 2023, there will be around 900,000 symptomatic and 5,000,000 asymptomatic cases (Figure 16A,B). In this graph, there is no decay regardless of the duration of the loss of immunity. For a 100-day

duration, cases will peak at roughly 532,546 symptomatic and 5 million asymptomatic cases, followed by a slight descent to stabilize at approximately 500,000 symptomatic and 4.5 million asymptomatic active cases (Figure 16A,B). For a 150-day duration, cases will peak at 450,000 and 3.2 million for symptomatic and asymptomatic active cases, respectively. Once a peak is reached, there is a modest descent and a stabilization in 400,000 and 2.4 million symptomatic and asymptomatic cases, respectively (Figure 16A,B). There is a noticeable difference in the size of the subsequent wave of COVID-19 influenced by the waning of immunity. Despite a considerable increase of infected cases, hospitalized individuals will rise, but not by a considerable amount. For a 50-day duration in the peak, there will be roughly 620,000 individuals; for 100-days, 350,000 individuals; and for 150-days, 220,000 individuals (Figure 16C). This modest increase in hospitalizations is a product of a population with a level of protection from the virus that influences a re-infection, but the infection does not produce severe COVID-19 due to a combination of immunity acquired by the vaccine or by a prior infection. The death toll is affected as well, with a decay of around 100,000 deaths with 50 days of protection when we compared with 100-days, and a difference of 50,000 difference between the cases with 150 and 100 days (Figure 16D).

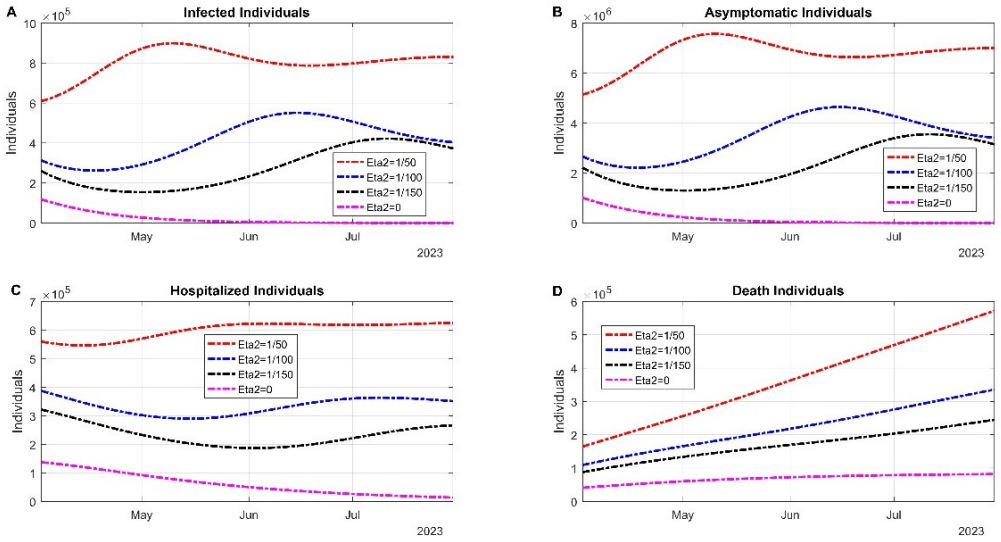

Figure 16. Dynamics of the population when the waning rate is varied between September and November 2022. A: Dynamics of the infected symptomatic individuals; B: asymptomatic infected individuals; C: variation of hospital admission; D: death toll of COVID-19. In all panels, the red dotted line means that the immunity wanes in 50 days, the blue dotted line in 100 days, the black dotted line in 150 days, and the pink dotted line denotes a sterilizing immunity.

3.7. Influence of the probability of re-infection prior to get infected with another Omicron sublineage on the pattern of new infections for the following months

Re-infection prior to get infected with another sublineage, or *cross immunity*, is defined as the immune response from one infection that will confer a protection from another infection. The following

waves may be affected by the existence of cross immunity. The third wave of COVID-19 in Mexico was heavily influenced by the presence of XBB, which affected the peak of cases when BQ.1 was introduced in the population [24]. Since a prior infection with XBB could affect a sudden re-infection with BQ.1, an important portion of the population had protection and may be infected in this wave, but the story can be different in the subsequent wave. Between January and April 2023, the peak was influenced by the value of immunity prior to infection with XBB: there was a reduction of approximately 140,000 active symptomatic cases and 1,200,000 asymptomatic cases, because they had a prior infection with XBB (Figure S13A,B). Hospitalizations and death toll also are affected by this cross-immunity between sublineages with a reduction of 80,000 hospitalizations and 20,000 fewer deaths due to the influence of prior XBB infection (Figure S13C,D).

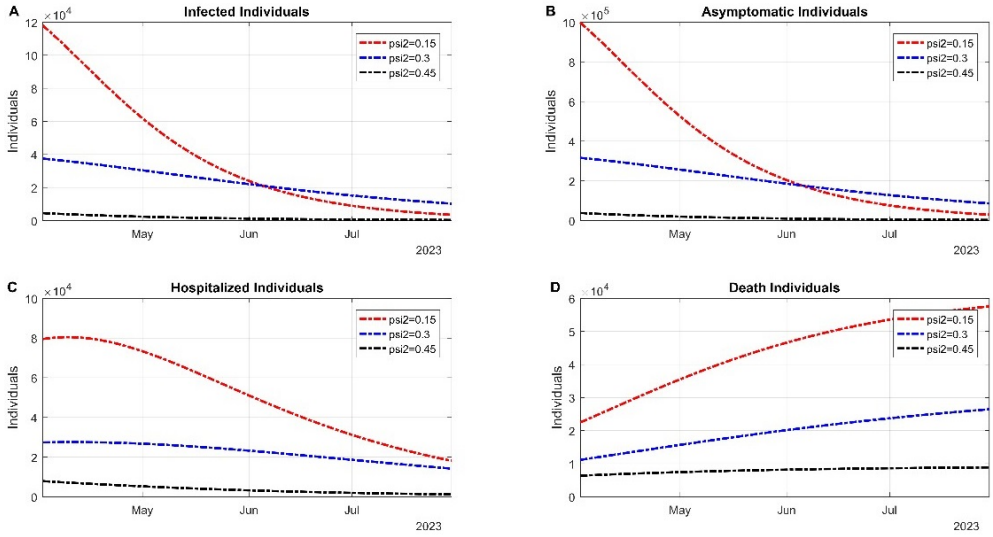

Figure 17. Dynamics of the population when the cross immunity is varied between September and November 2022. A: Dynamics of the infected symptomatic individuals; B: asymptomatic infected individuals; C: variation of hospital admission; D: death toll of COVID-19. In all panels, the red dotted line means that once infected we only have a 15% of protection, the blue dotted line indicates that we only have a 30% of protection, the black dotted line represents that we only have a 45% of protection.

For the third Omicron wave in the last month of 2022, the size of the peak and the time it takes to reach that peak are affected by a prior infection of XBB and BQ.1. A lower protection is associated to a peak of around 18,000 new infections with symptoms and 200,000 asymptomatic cases (Figure 17A,B). With baseline protection, the peak is reduced by 100,000 infections, and it takes just about a one and a half months to reach that peak compared with a lower protection, when it only three weeks to reach it (Figure 17). For the case of asymptomatic infections, there may a be reduction of approximately 10,000 active cases that were infected in the prior wave (Figure 17B). Hospitalizations are affected as well: for lower protection, there may be roughly 20,000 new hospitalizations during the second wave of 2023; instead, baseline protection may be associated with a decrease of 2000 infections, reaching 18,000 new hospitalizations between May and July 2023 (Figure 17C). Finally, the death toll is influenced by the prior infection with another sublineage: for a low protection, there may be roughly 60,000

deaths due to COVID-19; alternatively, baseline protection can significantly decrease the death toll, with a reduction of 30,000 deaths (Figure 17D). The protection, or how well the new variant avoids elimination by the immune system, can influence the the dynamics of the following waves of COVID-19, unless another variant arises where a previous infection with another sublineage no longer results in some type of protection.

3.8. Assessing the combined effect of face mask usage, face mask efficiency and efficiency of protection due to partial immunity in reducing the control reproduction number

In this section, we evaluate the importance of the use of face masks and the efficiency, combined with the efficiency of protection due to partial immunity, to reduce the control reproduction number. To take this into account, we rescale the transmission rates β_1, β_2, β_3, and β_4 by a factor $(1 - C_m\epsilon_m)$, where C_m denotes the proportion of the population that uses face masks and ϵ_m represents the efficiency of face masks.

Figure 18 depicts the values of the control reproduction number obtained using the baseline parameter values as before, for three different values of the protection due to partial immunity against sublineage BQ.1 (ψ_2). Since the reproduction number corresponding to sublineage XBB is lower than that of sublineage BQ.1, a variation in the value of the protection against the first sublineage (ψ_1) does not modify the value of the control reproduction number.

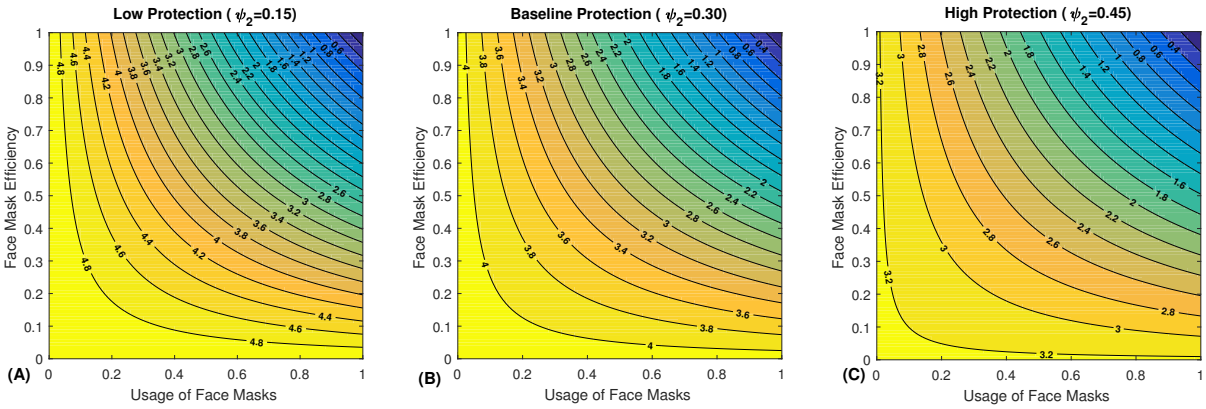

Figure 18. Contour plot of the control reproduction number as a function of the usage of face masks C_m and the face mask efficiency ϵ_m combined with the variation of protection due to partial immunity ψ_2. A: Low protection; B: baseline protection; C: high protection.

3.9. Local sensitivity analysis of the control reproduction number

To evaluate the sensitivity of the control reproduction number as each of the model parameters is varied, we computed the elasticity indices of $\mathcal{R}_c$ with respect to each parameter. Figure 19 shows the corresponding values for the parameters that have an elasticity index greater than zero. The proportion of symptomatic cases for sublineage BQ.1 (p_2) and the transmission rate of the same sublineage by contact with symptomatic individuals (β_3) have the largest importance on increasing the reproduction number; in comparison, the transmission rate by contact with asymptomatic individuals (β_4) has a very small importance. On the other hand, the most important parameter associated with a decrease in $\mathcal{R}_c$

is the recovery rate of infection by sublineage BQ.1 (γ_2). The protection against this sublineage given by partial immunity (either natural or vaccine-acquired), denoted by ψ_2, has a smaller, although still significant importance on decreasing it, and it is followed by the face mask usage C_m and face mask efficiency ϵ_m. The next most important parameters are the hospitalization rate (σ) and the proportion of hospitalized cases for sublineage BQ.1 (φ_2). The rest of the parameters have only a very small influence on the value of the control reproduction number.

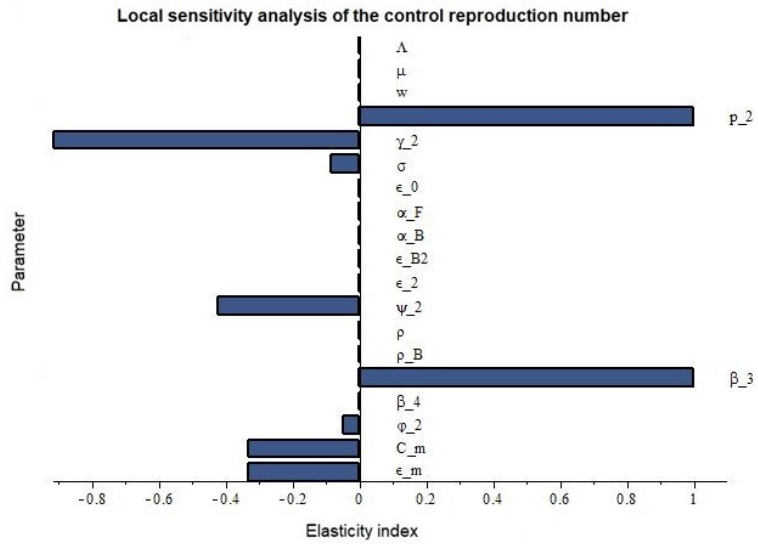

Figure 19. Local elasticity indices of the control reproduction number with respect to the model parameters. Parameters that do not change the value of $\mathcal{R}_c$ when locally perturbed are not shown.

4. Discussion

More than two years after the pandemic started, we are still using mathematical models to forecast the spread of SARS-CoV-2 and help inform public health decisions. In Mexico, the year 2022 was marked by the entry of Omicron into the population, mixed with the roll-out of boosters and the continuous use of face masks in open and closed places [44]. Despite the use of face masks in the population, the transmission was high when Omicron entered, which resulted in an exponential increase of newly infected individuals. As of January 2023, the population vaccinated against COVID-19 in Mexico was around 76% [45], meaning there is a sector of the population that was not vaccinated, with vaccine hesitancy being one of the most important reasons [46, 47].

In this work, we carried out a theoretical and numerical analysis for an epidemic model that can be used to analyze the dynamics of the Omicron wave and subsequent waves, as well as the impact of vaccination campaigns in Mexico. Our compartmentalized model considered the spread in the unvaccinated and vaccinated subpopulations to better portray the ongoing COVID-19 pandemic. We also considered the particular vaccine campaigns in Mexico with seven different vaccines against COVID-19, as well as how this heterogeneity affected the global dynamics of the spread of COVID-19. Furthermore, we considered the transmission and immunity parameters associated with the XBB and BQ.1 variants. Our population was divided into four important subpopulations:

unvaccinated (susceptible individuals), individuals vaccinated with only a two-dose scheme, individuals vaccinated with one or two boosters, and partially protected susceptible individuals (individuals with waning immunity, either acquired or natural). These subdivisions helped us understand which population will be the force for the subsequent Omicron waves if no other variant emerges and what public health decisions we need to face the following waves. Despite our model being constructed based on previous works and to our concern, there is no mathematical model applied in Mexico that introduces novelties such as vaccine heterogeneity, the inclusion of a hospitalized compartment, vaccine booster, the use of face masks and their related efficiencies, cross-immunity between Omicron sublineages, and modeling the waning of natural and acquired immunity as a two-stage process.

Face mask usage in the population and face mask efficiency are two important parameters with a large impact on the dynamics of the control reproduction number. We noted that N95 face masks are the most effective to reduce the spread and eliminate the pandemic, and this type of face mask is inexpensive based on the economy of this year [48]. The least effective face masks are cloth and improved cloth face masks, as expected. However, if 75% of the population used cloth face masks (30% efficiency), the new infections (symptomatic or not) can be reduced by 20%; while if 75% of the population uses an improved cloth face mask (50% efficiency), the transmission is reduced in 40% compared with no use of face masks. Surgical masks, which are a more suitable type of mask to purchase based on their cost, can reduce transmission by 64% compared with no use of face mask if 75% of the population wears them. If there are still people who do not want to wear face masks, with only 50% wearing surgical face masks, there is a 40% decrease in new cases, whether symptomatic or asymptomatic. Surgical face masks are the best option in terms of reduction in transmission and costs. Vaccines have reduced hospitalizations and therefore deaths [42], although they have not been able to reduce transmission between individuals. Our best strategy to reduce infections is the use of face masks [49, 50]. We highly recommend that the use of face masks continues until the end of 2023 to reduce the spread, but this can change based on the dynamics of the spread in the following months, combined with the possible emergence of a new sublineage of Omicron or a variant.

The application of multiple vaccines in Mexico has significantly helped to reduce hospitalizations and deaths, even though they were developed to combat the original Wuhan strain. Even so, the cross-protection efficiency is waning over time for vaccine-acquired, natural, or hybrid immunity [51, 52]. Our simulations showed an increase in new infections when we vary the immunity period between 50 days and 150 days, with the possibility of another Omicron BQ.1 wave between November and December 2022. The size of the following peak may be influenced by the loss of protection, either acquired or natural. If the loss of immunity were 50 days, there may be an increase of 50% in new infections. Furthermore, if we increase the loss of immunity to 150 days, the peak in November may be reduced by 10% compared with the baseline 100-day immunity period. The predicted peak will be 75% lower than the peak in July–August 2022. There is a possibility of another Omicron wave by May 2023, with a 40% reduction with respect to the wave in November–December 2022. The pattern of waning immunity will shape the behavior of following waves and how we will face the wave. Nevertheless, the application of a booster of bivalent vaccine that contains the ancestral Wuhan and the Omicron BA.1 in the fall may be a significant change in terms of loss of acquired immunity [53].

Cross-immunity is an important concept to be considered in a mathematical model that

incorporates two sublineages of the same variant [54]. This means that if someone gets infected with a prior sublineage or variant, they may have protection because of the vaccine-acquired or natural immunity. Since XBB was the main driver for the second wave in Mexico, we incorporated how cross-immunity affected the BQ.1 wave in Mexico and how it may affect subsequent waves. We were able to observe that, as the cross-immunity varied, the size of the next wave changed. With greater protection, the peak decreases compared to the case with less protection, a reduction of almost 25%. In addition, if there was a higher protection, the time to reach the peak would increase. Less protection implies that it takes a month and a half to reach the peak, while with greater protection it takes two months and a week to reach the peak. We highly suggest monitoring cross-immunity protection on a long-term scale to visualize possible subsequent waves of Omicron sublineages or multiple rolling strains.

5. Conclusions

In essence, our mathematical model provides a projection of the ongoing COVID-19 pandemic in Mexico, distinguishing new cases arising by the multiple vaccines applied in the vaccination campaign. We demonstrated that all vaccines applied, regardless of their vaccine efficiency against symptomatic COVID-19, have helped in reducing hospitalizations and deaths from COVID-19. We understand that this type of mathematical model is heavily influenced by social behavior, but it still can inform us to take important public health decisions. We recommend the continuous use of face masks in open and closed places with at least 50% efficiency protection against Omicron sublineage, at the minimum for the rest of the year. Finally, two important parameters will shape the behavior of the pandemic: waning immunity and cross-immunity between Omicron sublineages or with a possible emerging strain. We recommend monitoring these parameters and the way they affect the control reproduction number and herd immunity, as well as methods for controlling them using pharmaceutical or non-pharmaceutical strategies.

Use of AI tools declaration

The authors declare they have not used Artificial Intelligence (AI) tools in the creation of this article.

Acknowledgments

This article was supported in part by Mexican SNI under CVU 15284.

Data and materials availability

The original contributions presented in this study are included in the article–Supplementary material. All code used for analysis is available at https://github.com/UgoAvila/Mathematical-Model-of-COVID-19-in-Mexico-waning-and-cross-immunity.

Conflict of interest

The authors declare there is no conflict of interest.

References

1. E. Dong, H. Du, L. Gardner, An interactive web-based dashboard to track COVID-19 in real time, *Lancet Infect. Dis.*, **20** (2020), 533–534. https://doi.org/10.1016/S1473-3099(20)30120-1
2. E. Mathieu, H. Ritchie, L. Rodés-Guirao, C. Appel, C. Giattino, J. Hasell, et al., Coronavirus pandemic (COVID-19), Our World in Data. Available from: https://ourworldindata.org/coronavirus.
3. Secretaría de Salud, Sana distancia COVID-19, Gobierno de México. Available from: https://www.gob.mx/salud/documentos/sana-distancia.
4. Gobierno de México, Semáforo COVID-19. Available from: https://web.archive.org/web/20220630213907/https://coronavirus.gob.mx/semaforo/.
5. Comisión Federal para la Protección contra Riesgos Sanitarios, Vacunas COVID 19 autorizadas, Gobierno de México. Available from: https://www.gob.mx/cofepris/acciones-y-programas/vacunas-covid-19-autorizadas.
6. L. Matrajt, J. Eaton, T. Leung, E. R. Brown, Vaccine optimization for COVID-19: Who to vaccinate first, *Sci. Adv.*, **7** (2021), eabf1374. https://doi.org/10.1126/sciadv.abf1374
7. K. M. Bubar, K. Reinholt, S. M. Kissler, M. Lipsitch, S. Cobey, Y. H. Grad, et al., Model-informed COVID-19 vaccine prioritization strategies by age and serostatus, *Science*, **371** (2021), 916–921. https://doi.org/10.1126/science.abe6959
8. Secretaría de Salud, Vacuna Covid–Sitio informativo. Available from: https://web.archive.org/web/20220808220248/http://vacunacovid.gob.mx/wordpress/.
9. M. M. Alvarez, S. Bravo-González, G. Trujillo-de Santiago, Modeling vaccination strategies in an Excel spreadsheet: Increasing the rate of vaccination is more effective than increasing the vaccination coverage for containing COVID-19, *PLoS One*, **16** (2021), e0254430. https://doi.org/10.1371/journal.pone.0254430
10. A. del C. Munguía-López, J. M. Ponce-Ortega, Fair allocation of potential COVID-19 vaccines using an optimization-based strategy, *Process Integr. Optim. Sustainability*, **5** (2021), 3–12. https://doi.org/10.1007/s41660-020-00141-8
11. I. Soria-Arguello, R. Torres-Escobar, H. A. Pérez-Vicente, T. G. Perea-Rivera, A proposal mathematical model for the vaccine COVID-19 distribution network: A case study in Mexico, *Math. Probl. Eng.*, **2021** (2021), 5484101. https://doi.org/10.1155/2021/5484101
12. F. Saldaña, J. X. Velasco-Hernández, The trade-off between mobility and vaccination for COVID-19 control: A metapopulation modelling approach, *Royal Soc. Open Sci.*, **8** (2021), 202240. https://doi.org/10.1098/rsos.202240
13. A. S. Lauring, E. B. Hodcroft, Genetic variants of SARS-CoV-2—What do they mean, *JAMA*, **325** (2021), 529–531. https://doi.org/10.1001/jama.2020.27124

14. A. M. Gravagnuolo, L. Faqih, C. Cronshaw, J. Wynn, L. Burglin, P. Klapper, et al., Epidemiological investigation of new SARS-CoV-2 variant of concern 202012/01 in England, preprint, medRxiv:2021.01.14.21249386.

15. S. Zárate, B. Taboada, J. E. Muñoz-Medina, P. Iša, A. Sanchez-Flores, C. Boukadida, et al., The Alpha variant (B.1.1.7) of SARS-CoV-2 failed to become dominant in Mexico, *Microbiol. Spectrum*, **10** (2022), e02240–21. https://doi.org/10.1128/spectrum.02240-21

16. B. Taboada, S. Zárate, P. Iša, C. Boukadida, J. A. Vazquez-Perez, J. E. Muñoz-Medina, et al., Genetic analysis of SARS-CoV-2 variants in Mexico during the first year of the COVID-19 pandemic, *Viruses*, **13** (2021), 2161. https://doi.org/10.3390/v13112161

17. B. Taboada, S. Zárate, R. García-López, J. E. Muñoz-Medina, A. Sanchez-Flores, A. Herrera-Estrella, et al., Dominance of three sublineages of the SARS-CoV-2 Delta variant in Mexico, *Viruses*, **14** (2022), 1165. https://doi.org/10.3390/v14061165

18. S. Mallapaty, Where did Omicron come from? Three key theories, *Nature*, **602** (2022), 26–28. https://doi.org/10.1038/d41586-022-00215-2

19. R. Viana, S. Moyo, D. G. Amoako, H. Tegally, C. Scheepers, C. L. Althaus, et al., Rapid epidemic expansion of the SARS-CoV-2 Omicron variant in southern Africa, *Nature*, **603** (2022), 679–686. https://doi.org/10.1038/s41586-022-04411-y

20. H. Gruell, K. Vanshylla, P. Tober-Lau, D. Hillus, P. Schommers, C. Lehmann, et al., mRNA booster immunization elicits potent neutralizing serum activity against the SARS-CoV-2 Omicron variant, *Nat. Med.*, **28** (2022), 477–480. https://doi.org/10.1038/s41591-021-01676-0

21. K. Khan, F. Karim, Y. Ganga, M. Bernstein, Z. Jule, K. Reedoy, et al., Omicron sub-lineages BA.4/BA.5 escape neutralizing immunity elicited by BA.1 infection, *Nat. Commun.*, **13** (2022), 4686. https://doi.org/10.1038/s41467-022-32396-9

22. Outbreak.info, SARS-CoV-2 (hCoV-19) mutation reports–lineage comparison, Enabled by data from GISAID. Available from: https://outbreak.info/compare-lineages?pango=BA.5&pango=BA.4&pango=BA.2.12.1&pango=BA.2&pango=BA.1&gene=ORF1a&gene=ORF1b&gene=S&gene=ORF3a&gene=E&gene=M&gene=ORF6&gene=ORF7a&gene=ORF7b&gene=ORF8&gene=N&gene=ORF10&threshold=75&nthresh=1&sub=false&dark=true.

23. H. N. Altarawneh, H. Chemaitelly, H. Ayoub, M. R. Hasan, P. Coyle, H. M. Yassine, et al., Protection of SARS-CoV-2 natural infection against reinfection with the BA.4 or BA.5 Omicron subvariants, preprint, medRxiv:10.1101/2022.07.11.22277448.

24. MexCoV2, Consorcio Mexicano de Vigilancia Genómica, (CoViGen-Mex). Available from: http://mexcov2.ibt.unam.mx:8080/COVID-TRACKER/.

25. Gobierno de México, Secretaría de Salud abre registro para vacuna de refuerzo a personas de 30 a 39 años, Secretaría de Salud. Available from: https://www.gob.mx/salud/prensa/056-secretaria-de-salud-abre-registro-para-vacuna-de-refuerzo-a-personas-de-30-a-39-anos.

26. L. Benahmadi, M. Lhous, A. Tridane, O. Zakary, M. Rachik, Modeling the impact of the imperfect vaccination of the COVID-19 with optimal containment strategy, *Axioms*, **11** (2022), 124. https://doi.org/10.3390/axioms11030124

27. C. J. Edholm, B. Levy, L. Spence, F. B. Agusto, F. Chirove, C. W. Chukwu, et al., A vaccination model for COVID-19 in Gauteng, South Africa, *Infect. Dis. Modell.*, **7** (2022), 333–345. https://doi.org/10.1016/j.idm.2022.06.002

28. G. G. Parra, A. J. Arenas, A nonlinear mathematical model for the dynamics of the Omicron wave, preprint, SSRN:4119450. https://doi.org/10.2139/ssrn.4119450

29. S. Safdar, C. N. Ngonghala, A. Gumel, Mathematical assessment of the role of waning and boosting immunity against the BA.1 Omicron variant in the United States, *Math. Biosci. Eng.*, **20** (2023), 179–212. https://doi.org/10.3934/mbe.2023009

30. K. Koelle, M. A. Martin, R. Antia, B. Lopman, N. E. Dean, The changing epidemiology of SARS-CoV-2, *Science*, **375** (2022), 1116–1121. https://doi.org/10.1126/science.abm4915

31. A. G. C. Pérez, D. A. Oluyori, An extended SEIARD model for COVID-19 vaccination in Mexico: Analysis and forecast, *Math. Appl. Sci. Eng.*, **2** (2021), 219–309. https://doi.org/10.5206/mase/14233

32. F. J. Aguilar-Canto, U. Avila-Ponce de León, E. Avila-Vales, Sensitivity theorems of a model of multiple imperfect vaccines for COVID-19, *Chaos Solitons Fractals*, **156** (2022), 111844. https://doi.org/10.1016/j.chaos.2022.111844

33. F. M. G. Magpantay, Vaccine impact in homogeneous and age-structured models, *J. Math. Biol.*, **75** (2017), 1591–1617. https://doi.org/10.1007/s00285-017-1126-5

34. D. A. Swan, A. Goyal, C. Bracis, M. Moore, E. Krantz, E. Brown, et al., Mathematical modeling of vaccines that prevent SARS-CoV-2 transmission, *Viruses*, **13** (2021), 1921. https://doi.org/10.3390/v13101921

35. U. Avila-Ponce de León, E. Avila-Vales, K. L. Huang, Modeling COVID-19 dynamic using a two-strain model with vaccination, *Chaos Solitons Fractals*, **157** (2022), 111927. https://doi.org/10.1016/j.chaos.2022.111927

36. Johns Hopkins CSSE, 2019 Novel Coronavirus COVID-19 (2019-nCoV) Data Repository. Available from: https://github.com/CSSEGISandData/COVID-19.

37. Institute for Health Metrics and Evaluation, COVID-19 estimate downloads. Available from: https://www.healthdata.org/covid/data-downloads.

38. Our World in Data, Coronavirus (COVID-19) vaccinations. Available from: https://github.com/owid/covid-19-data/tree/master/public/data/vaccinations.

39. P. van den Driessche, J. Watmough, Reproduction numbers and sub-threshold endemic equilibria for compartmental models of disease transmission, *Math. Biosci.*, **180** (2002), 29–48. https://doi.org/10.1016/S0025-5564(02)00108-6

40. H. S. Rodrigues, M. T. T. Monteiro, D. F. M. Torres, Sensitivity analysis in a dengue epidemiological model, *Conf. Pap. Sci.*, **2013** (2013), 721406. https://doi.org/10.1155/2013/721406

41. World Health Organization, Global COVID-19 vaccination strategy in a changing world: July 2022 update. Available from: https://www.who.int/publications/m/item/global-covid-19-vaccination-strategy-in-a-changing-world–july-2022-update.

42. O. J. Watson, G. Barnsley, J. Toor, A. B. Hogan, P. Winskill, A. C. Ghani, Global impact of the first year of COVID-19 vaccination: A mathematical modelling study, *Lancet Infect. Dis.*, **22** (2022), 1293–1302. https://doi.org/10.1016/S1473-3099(22)00320-6
43. Gobierno de México, Gestión diplomática sobre vacunas COVID-19. Available from: https://portales.sre.gob.mx/transparencia/gestion-diplomatica-vacunas-covid.
44. Secretaría de Salud, Uso del cubreboca COVID-19, Gobierno de México. Available from: https://www.gob.mx/salud/documentos/uso-del-cubreboca?state=published.
45. E. Mathieu, H. Ritchie, E. Ortiz-Ospina, M. Roser, J. Hasell, C. Appel, et al., A global database of COVID-19 vaccinations, *Nat. Hum. Behav.*, **5** (2021), 947–953. https://doi.org/10.1038/s41562-021-01122-8
46. V. C. Lucia, A. Kelekar, N. M. Afonso, COVID-19 vaccine hesitancy among medical students, *J. Public Health*, **43** (2021), 445–449. https://doi.org/10.1093/pubmed/fdaa230
47. S. Machingaidze, C. S. Wiysonge, Understanding COVID-19 vaccine hesitancy, *Nat. Med.*, **27** (2021), 1338–1339. https://doi.org/10.1038/s41591-021-01459-7
48. J. A. Carrillo, A. L. García, The COVID-19 economic crisis in Mexico through the lens of a financial conditions index, *Lat. Am. Econ. Rev.*, **30** (2021), 1–27. https://doi.org/10.47872/laer.v30.41
49. J. Howard, A. Huang, Z. Li, Z. Tufekci, V. Zdimal, H. M. van der Westhuizen, et al., An evidence review of face masks against COVID-19, *Proc. Natl. Acad. Sci.*, **118** (2021), e2014564118. https://doi.org/10.1073/pnas.2014564118
50. G. Leech, C. Rogers-Smith, J. T. Monrad, J. B. Sandbrink, B. Snodin, R. Zinkov, et al., Mask wearing in community settings reduces SARS-CoV-2 transmission, *Proc. Natl. Acad. Sci.*, **119** (2022), e2119266119. https://doi.org/10.1073/pnas.2119266119
51. C. Willyard, What the Omicron wave is revealing about human immunity, *Nature*, **602** (2022), 22–25. https://doi.org/10.1038/d41586-022-00214-3
52. I. Kislaya, P. Casaca, V. Borges, C. Sousa, B. I. Ferreira, A. Fonte, et al., Comparative COVID-19 vaccines effectiveness in preventing infections, hospitalizations, and deaths with SARS-CoV-2 BA.5 and Ba.2 Omicron lineages: A case-case and cohort study using electronic health records in Portugal, preprint, SSRN:4180482. https://doi.org/10.2139/ssrn.4180482
53. S. Chalkias, C. Harper, K. Vrbicky, S. R. Walsh, B. Essink, A. Brosz, et al., A bivalent Omicron-containing booster vaccine against Covid-19, *New Engl. J. Med.*, **387** (2022), 1279–1291. https://doi.org/10.1056/NEJMoa2208343
54. S. Bhattacharyya, P. H. Gesteland, K. Korgenski, O. N. Bjørnstad, F. R. Adler, Cross-immunity between strains explains the dynamical pattern of paramyxoviruses, *Proc. Natl. Acad. Sci.*, **112** (2015), 13396–13400. https://doi.org/10.1073/pnas.1516698112

Appendix

A1. Mathematical model with asymptomatic individuals, vaccination, waning immunity, and cross-immunity protection between sublineages

The model studied here is described by the following system of differential equations:

$$
\begin{aligned}
\frac{dS}{dt} &= \Lambda - \left(\frac{\beta_1 I_1 + \beta_2 A_1}{X}\right) S - \left(\frac{\beta_3 I_2 + \beta_4 A_2}{X}\right) S - \varepsilon_0 \rho S - \mu S,\\
\frac{dF}{dt} &= \varepsilon_0 \rho S - \mathcal{E}_1 \left(\frac{\beta_1 I_1 + \beta_2 A_1}{X}\right) F - \mathcal{E}_2 \left(\frac{\beta_3 I_2 + \beta_4 A_2}{X}\right) F - \alpha_F F - \rho_B F - \mu F,\\
\frac{dB}{dt} &= \rho_B F - (1-\varepsilon_{B1}) \left(\frac{\beta_1 I_1 + \beta_2 A_1}{X}\right) B - (1-\varepsilon_{B2}) \left(\frac{\beta_3 I_2 + \beta_4 A_2}{X}\right) B - \alpha_B B - \mu B,\\
\frac{dE_1}{dt} &= \left(\frac{\beta_1 I_1 + \beta_2 A_1}{X}\right) S + (1-\psi_1) \left(\frac{\beta_1 I_1 + \beta_2 A_1}{X}\right) S_p + \mathcal{E}_1 \left(\frac{\beta_1 I_1 + \beta_2 A_1}{X}\right) F\\
&\quad + (1-\varepsilon_{B1}) \left(\frac{\beta_1 I_1 + \beta_2 A_1}{X}\right) B - w E_1 - \mu E_1,\\
\frac{dI_1}{dt} &= p_1 w E_1 - \gamma_1 (1-\varphi_1) I_1 - \sigma \varphi_1 I_1 - \mu I_1,\\
\frac{dA_1}{dt} &= (1-p_1) w E_1 - \gamma_1 A_1 - \mu A_1,\\
\frac{dH_1}{dt} &= \sigma \varphi_1 I_1 - \omega_1 H_1 - \mu H_1,\\
\frac{dR_1}{dt} &= \gamma_1 (1-\varphi_1) I_1 + \gamma_1 A_1 + \omega_1 (1-\chi_1) H_1 - \eta_1 R_1 - \mu R_1,\\
\frac{dS_p}{dt} &= \alpha_F F + \alpha_B B + \eta_1 R_1 + \eta_2 R_2 - (1-\psi_1) \left(\frac{\beta_1 I_1 + \beta_2 A_1}{X}\right) S_p\\
&\quad - (1-\psi_2) \left(\frac{\beta_3 I_2 + \beta_4 A_2}{X}\right) S_p - \mu S_p,\\
\frac{dE_2}{dt} &= \left(\frac{\beta_3 I_2 + \beta_4 A_2}{X}\right) S + (1-\psi_2) \left(\frac{\beta_3 I_2 + \beta_4 A_2}{X}\right) S_p + \mathcal{E}_2 \left(\frac{\beta_3 I_2 + \beta_4 A_2}{X}\right) F\\
&\quad + (1-\varepsilon_{B2}) \left(\frac{\beta_3 I_2 + \beta_4 A_2}{X}\right) B - w E_2 - \mu E_2,\\
\frac{dI_2}{dt} &= p_2 w E_2 - \gamma_2 (1-\varphi_2) I_2 - \sigma \varphi_2 I_2 - \mu I_2,\\
\frac{dA_2}{dt} &= (1-p_2) w E_2 - \gamma_2 A_2 - \mu A_2,\\
\frac{dH_2}{dt} &= \sigma \varphi_2 I_2 - \omega_2 H_2 - \mu H_2,\\
\frac{dR_2}{dt} &= \gamma_2 (1-\varphi_2) I_2 + \gamma_2 A_2 + \omega_2 (1-\chi_2) H_2 - \eta_2 R_2 - \mu R_2,\\
\frac{dD_1}{dt} &= \omega_1 \chi_1 H_1,\\
\frac{dD_2}{dt} &= \omega_2 \chi_2 H_2,
\end{aligned}
\tag{A1.1}
$$

where

$$\varepsilon_0 = \sum_{i=1}^{3}(1-\varepsilon_{ai})w_i, \qquad \mathcal{E}_1 = \frac{1}{3}\sum_{i=1}^{3}(1-\varepsilon_{1i}), \qquad \mathcal{E}_2 = \frac{1}{3}\sum_{i=1}^{3}(1-\varepsilon_{2i}),$$

$$X = S + F + B + E_1 + I_1 + A_1 + H_1 + R_1 + S_p + E_2 + I_2 + A_2 + H_2 + R_2,$$

and the variables have the following meaning:

- S: unvaccinated susceptible individuals.
- F: individuals vaccinated with at least one dose but no booster doses.
- B: individuals vaccinated with at least one booster dose.
- E_1: individuals exposed to sublineage 1 Omicron.
- I_1: symptomatic individuals infected with sublineage 1 Omicron.
- A_1: asymptomatic individuals infected with sublineage 1 Omicron.
- H_1: hospitalized with sublineage 1 Omicron.
- R_1: recovered after infection with sublineage 1 Omicron.
- S_p: susceptible individuals with partial immunity.
- E_2: exposed individuals to sublineage 2 Omicron.
- I_2: symptomatic individuals infected with sublineage 2 Omicron.
- A_2: asymptomatic individuals infected with sublineage 2 Omicron.
- H_2: hospitalized with sublineage 2 Omicron.
- R_2: recovered after infection with sublineage 2 Omicron.
- D_1: cumulative number of deaths due to sublineage 1 Omicron.
- D_2: cumulative number of deaths due to sublineage 2 Omicron.

A2. Mathematical analysis

A2.1. Boundedness of the system

It is readily verified that every solution of system (A1.1) with non-negative initial conditions remains non-negative for all $t \geq 0$. Let $X = S + F + B + E_1 + I_1 + A_1 + H_1 + R_1 + S_p + E_2 + I_2 + A_2 + H_2 + R_2$. Then,

$$\begin{aligned}\frac{dX}{dt} &= \frac{dS}{dt} + \frac{dF}{dt} + \frac{dB}{dt} + \frac{dE_1}{dt} + \frac{dI_1}{dt} + \frac{dA_1}{dt} + \frac{dH_1}{dt} + \frac{dR_1}{dt} + \frac{dS_p}{dt} + \frac{dE_2}{dt} + \frac{dI_2}{dt} + \frac{dA_2}{dt} + \frac{dH_2}{dt} + \frac{dR_2}{dt} \\ &= \Lambda - \mu X - (\omega_2\chi_2 H_2 + \omega_1\chi_1 H_1),\end{aligned}$$

which implies

$$\frac{dX}{dt} + \mu X = \Lambda - (\omega_1\chi_1 H_1 + \omega_2\chi_2 H_2).$$

Since $-(\omega_1\chi_1 H_1 + \omega_2\chi_2 H_2) \leq 0$,

$$\frac{dX}{dt} + \mu X \leq \Lambda.$$

Using the integrating factor

$$e^{\int \mu\, dt} = e^{\mu t},$$

we get

$$\begin{aligned} & e^{\mu t}\frac{dX}{dt} + \mu e^{\mu t}X \leq \Lambda e^{\mu t} \\ \Longrightarrow\ & \frac{d}{dt}(e^{\mu t}X) \leq \Lambda e^{\mu t} \\ \Longrightarrow\ & e^{\mu t}X \leq \int \Lambda e^{\mu t}\, dt \\ \Longrightarrow\ & e^{\mu t}X \leq \Lambda\left(\frac{e^{\mu t}}{\mu} + c\right) \\ \Longrightarrow\ & X \leq \frac{\Lambda}{\mu} + c\Lambda e^{-\mu t}. \end{aligned}$$

If we let $t \to \infty$, we obtain

$$\limsup_{t\to\infty} X \leq \frac{\Lambda}{\mu}$$

hence, all the solutions of (A1.1) initiating in $\left\{\mathbb{R}^{10}_{+} \setminus \{0\}\right\}$ are confined to the region

$$\mathbf{R} = \left\{(S, F, B, E_1, I_1, A_1, H_1, R_1, S_p, E_2, I_2, A_2, H_2, R_2) \in \mathbb{R}^{14}_{+} : X \leq \frac{\Lambda}{\mu} + \epsilon\right\}$$

for any $\epsilon > 0$ and for $t \to \infty$.

A2.2. Equilibria

We will proceed to find the equilibria of system (A1.1). First, let us notice that D_1 and D_2 are not in the other compartments, so we can omit them from the system. Now, we will equalize to zero $\frac{dS}{dt}, \frac{dF}{dt}, \frac{dB}{dt}, \frac{dE_1}{dt}, \frac{dI_1}{dt}, \frac{dA_1}{dt}, \frac{dH_1}{dt}, \frac{dR_1}{dt}, \frac{dS_p}{dt}, \frac{dE_2}{dt}, \frac{dI_2}{dt}, \frac{dA_2}{dt}, \frac{dH_2}{dt}, \frac{dR_2}{dt}$, obtaining

$$0 = \Lambda - \left(\frac{\beta_1 I_1 + \beta_2 A_1}{X}\right)S - \left(\frac{\beta_3 I_2 + \beta_4 A_2}{X}\right)S - \varepsilon_0\rho S - \mu S, \tag{A2.1}$$

$$0 = \varepsilon_0\rho S - \mathcal{E}_1\left(\frac{\beta_1 I_1 + \beta_2 A_1}{X}\right)F - \mathcal{E}_2\left(\frac{\beta_3 I_2 + \beta_4 A_2}{X}\right)F - \alpha_F F - \rho_B F - \mu F, \tag{A2.2}$$

$$0 = \rho_B F - (1-\varepsilon_{B1})\left(\frac{\beta_1 I_1 + \beta_2 A_1}{X}\right)B - (1-\varepsilon_{B2})\left(\frac{\beta_3 I_2 + \beta_4 A_2}{X}\right)B - \alpha_B B - \mu B, \tag{A2.3}$$

$$\begin{aligned} 0 = {} & \left(\frac{\beta_1 I_1 + \beta_2 A_1}{X}\right)S + (1-\psi_1)\left(\frac{\beta_1 I_1 + \beta_2 A_1}{X}\right)S_p + \mathcal{E}_1\left(\frac{\beta_1 I_1 + \beta_2 A_1}{X}\right)F \\ & + (1-\varepsilon_{B1})\left(\frac{\beta_1 I_1 + \beta_2 A_1}{X}\right)B - wE_1 - \mu E_1, \end{aligned} \tag{A2.4}$$

$$0 = p_1 wE_1 - \gamma_1(1-\varphi_1)I_1 - \sigma\varphi_1 I_1 - \mu I_1, \tag{A2.5}$$

$$0 = (1-p_1)wE_1 - \gamma_1 A_1 - \mu A_1, \tag{A2.6}$$

$$0 = \sigma\varphi_1 I_1 - \omega_1 H_1 - \mu H_1, \tag{A2.7}$$

$$0 = \gamma_1(1-\varphi_1)I_1 + \gamma_1 A_1 + \omega_1(1-\chi_1)H_1 - \eta_1 R_1 - \mu R_1, \tag{A2.8}$$

$$0 = \alpha_F F + \alpha_B B + \eta_1 R_1 + \eta_2 R_2 - (1-\psi_1)\left(\frac{\beta_1 I_1 + \beta_2 A_1}{X}\right) S_p \tag{A2.9}$$
$$- (1-\psi_2)\left(\frac{\beta_3 I_2 + \beta_4 A_2}{X}\right) S_p - \mu S_p,$$
$$0 = \left(\frac{\beta_3 I_2 + \beta_4 A_2}{X}\right) S + (1-\psi_2)\left(\frac{\beta_3 I_2 + \beta_4 A_2}{X}\right) S_p + \mathcal{E}_2 \left(\frac{\beta_3 I_2 + \beta_4 A_2}{X}\right) F \tag{A2.10}$$
$$+ (1-\varepsilon_{B2})\left(\frac{\beta_3 I_2 + \beta_4 A_2}{X}\right) B - wE_2 - \mu E_2,$$
$$0 = p_2 w E_2 - \gamma_2 (1-\varphi_2) I_2 - \sigma\varphi_2 I_2 - \mu I_2, \tag{A2.11}$$
$$0 = (1-p_2) w E_2 - \gamma_2 A_2 - \mu A_2, \tag{A2.12}$$
$$0 = \sigma\varphi_2 I_2 - \omega_2 H_2 - \mu H_2, \tag{A2.13}$$
$$0 = \gamma_2 (1-\varphi_2) I_2 + \gamma_2 A_2 + \omega_2 (1-\chi_2) H_2 - \eta_2 R_2 - \mu R_2, \tag{A2.14}$$

If we add all the equations, we obtain

$$\Lambda = \mu X + (\omega_1 \chi_1 H_1 + \omega_2 \chi_2 H_2),$$

and thus

$$\frac{\Lambda - \omega_1 \chi_1 H_1 - \omega_2 \chi_2 H_2}{\mu} = X \tag{A2.15}$$

A2.2.1. The disease-free equilibrium

If $I_1 = I_2 = 0$, it follows from Eq (A2.5) that $p_1 w E_1 = 0$, so $E_1 = 0$. In consequence, by (A2.6),

$$0 = -(\gamma_1 + \mu) A_1.$$

Then, $A_1 = 0$. It follows from (A2.7) that

$$0 = -(\omega_1 + \mu) H_1.$$

Then, $H_1 = 0$. From (A2.8),

$$-\eta_1 R_1 = 0.$$

Thus, $R_1 = 0$. A similar argument, using $I_2 = 0$ with Eqs (A2.11)–(A2.14) tells us that $E_2 = A_2 = H_2 = R_2 = 0$.

In consequence, the system is reduced to

$$0 = \Lambda - (\varepsilon_0 \rho + \mu) S, \tag{A2.16}$$
$$0 = \varepsilon_0 \rho S - (\alpha_F + \rho_B + \mu) F, \tag{A2.17}$$
$$0 = \rho_B F - (\alpha_B + \mu) B, \tag{A2.18}$$
$$0 = \alpha_F F + \alpha_B B - \mu S_p. \tag{A2.19}$$

By (A2.16),

$$S = \frac{\Lambda}{\varepsilon_0 \rho + \mu}.$$

Substituting in (A2.17) and simplifying, we get

$$F = \frac{\varepsilon_0 \rho \Lambda}{(\varepsilon_0 \rho + \mu)(\alpha_F + \rho_B + \mu)}. \tag{A2.20}$$

Using (A2.20) in (A2.18), we have

$$B = \frac{\varepsilon_0 \rho \rho_B \Lambda}{(\varepsilon_0 \rho + \mu)(\alpha_F + \rho_B + \mu)(\alpha_B + \mu)}. \tag{A2.21}$$

Last, substituting (A2.20) and (A2.21) in (A2.19) yields

$$S_p = \frac{\alpha_F \varepsilon_0 \rho \Lambda}{\mu(\varepsilon_0 \rho + \mu)(\alpha_F + \rho_B + \mu)} + \frac{\alpha_B \varepsilon_0 \rho \rho_B \Lambda}{\mu(\varepsilon_0 \rho + \mu)(\alpha_F + \rho_B + \mu)(\alpha_B + \mu)}.$$

Therefore, the disease-free equilibrium E_0 takes the form

$$E_0 = (S^0, F^0, B^0, 0, 0, 0, 0, 0, S_p^0, 0, 0, 0, 0, 0),$$

where

$$S^0 = \frac{\Lambda}{\varepsilon_0 \rho + \mu}, \qquad F^0 = \frac{\varepsilon_0 \rho \Lambda}{(\varepsilon_0 \rho + \mu)(\alpha_F + \rho_B + \mu)}, \qquad B^0 = \frac{\varepsilon_0 \rho \rho_B \Lambda}{(\varepsilon_0 \rho + \mu)(\alpha_F + \rho_B + \mu)(\alpha_B + \mu)},$$
$$S_p^0 = \frac{\varepsilon_0 \rho \Lambda}{\mu(\varepsilon_0 \rho + \mu)(\alpha_F + \rho_B + \mu)} \left(\alpha_F + \frac{\alpha_B \rho_B}{\alpha_B + \mu} \right).$$

A2.2.2. Endemic equilibrium

From (A2.5), we have

$$E_1 = \frac{I_1[\gamma_1(1 - \varphi_1) + \sigma\varphi_1 + \mu]}{p_1 w}. \tag{A2.22}$$

Substituting (A2.22) in (A2.6), we get

$$A_1 = \frac{I_1(1 - p_1)[\gamma_1(1 - \varphi_1) + \sigma\varphi_1 + \mu]}{p_1(\gamma_1 + \mu)}. \tag{A2.23}$$

From (A2.7),

$$H_1 = \frac{\sigma\varphi_1 I_1}{\omega_1 + \mu}. \tag{A2.24}$$

Substituting (A2.22)–(A2.24) in (A2.8), we obtain

$$R_1 = \frac{(G_1 + G_2 + G_3)\, I_1}{p_1(\eta_1 + \mu)D_1},$$

where

$$G_1 = p_1\gamma_1(1 - \varphi_1)(\omega_1 + \mu)(\gamma_1 + \mu),$$
$$G_2 = \gamma_1(1 - p_1)[\gamma_1(1 - \varphi_1) + \sigma\varphi_1 + \mu](\omega_1 + \mu),$$
$$G_3 = \sigma\omega_1\varphi_1 p_1(1 - \chi_1)(\gamma_1 + \mu),$$

$$D_1 = (\omega_1 + \mu)(\gamma_1 + \mu).$$

Analogously, we obtain

$$E_2 = \frac{I_2[\gamma_2(1-\varphi_2) + \sigma\varphi_2 + \mu]}{p_2 w},$$

$$A_2 = \frac{I_2(1-p_2)[\gamma_2(1-\varphi_2) + \sigma\varphi_2 + \mu]}{p_2(\gamma_2 + \mu)}, \tag{A2.25}$$

$$H_2 = \frac{\sigma\varphi_2 I_2}{\omega_2 + \mu}, \tag{A2.26}$$

and

$$R_2 = \frac{\left(G_1' + G_2' + G_3'\right) I_2}{p_2(\eta_2 + \mu)D_1'},$$

where

$$G_1' = p_2\gamma_2(1-\varphi_2)(\omega_2 + \mu)(\gamma_2 + \mu),$$

$$G_2' = \gamma_2(1-p_2)[\gamma_2(1-\varphi_2) + \sigma\varphi_2 + \mu](\omega_2 + \mu),$$

$$G_3' = \sigma\omega_2\varphi_2 p_2(1-\chi_2)(\gamma_2 + \mu),$$

$$D_1' = (\omega_2 + \mu)(\gamma_2 + \mu).$$

Substituting (A2.24) and (A2.26) in (A2.15), we obtain

$$X = \frac{\Lambda D_0 - \sigma I_1 D_2 - \sigma I_2 D_3}{\mu D_0}, \tag{A2.27}$$

where $D_0 = (\omega_1 + \mu)(\omega_2 + \mu)$, $D_2 = \omega_1\chi_1\varphi_1(\omega_2 + \mu)$, and $D_3 = \omega_2\chi_2\varphi_2(\omega_1 + \mu)$. Notice that, for the equilibrium to be positive, we require that $\mathcal{G}(I_1, I_2) > 0$, where $\mathcal{G}$ is defined by

$$\mathcal{G} = \mathcal{G}(I_1, I_2) := \Lambda D_0 - \sigma(I_1 D_2 + I_2 D_3). \tag{A2.28}$$

From (A2.1),

$$S = \frac{\Lambda X}{\beta_1 I_1 + \beta_2 A_1 + \beta_3 I_2 + \beta_4 A_2 + (\varepsilon_0\rho + \mu)X}.$$

Substituting (A2.23), (A2.25), and (A2.27), we obtain

$$S = \frac{\Lambda\mathcal{G}}{(\varepsilon_0\rho + \mu)\mathcal{G} + \mu D_0\left(I_1 G_4 + I_2 G_4'\right)}, \tag{A2.29}$$

where

$$G_4 = \beta_1 + \beta_2\frac{(1-p_1)[\gamma_1(1-\varphi_1) + \sigma\varphi_1 + \mu]}{p_1(\gamma_1 + \mu)},$$

$$G_4' = \beta_3 + \beta_4\frac{(1-p_2)[\gamma_2(1-\varphi_2) + \sigma\varphi_2 + \mu]}{p_2(\gamma_2 + \mu)}.$$

From (A2.2),

$$F = \frac{\varepsilon_0\rho X S}{\mathcal{E}_1(\beta_1 I_1 + \beta_2 A_1) + \mathcal{E}_2(\beta_3 I_2 + \beta_4 A_2) + (\alpha_F + \rho_B + \mu)X}.$$

Substituting (A2.23), (A2.25), (A2.27), and (A2.29) gives us

$$F = \frac{\varepsilon_0 \rho \Lambda \mathcal{G}^2}{[(\varepsilon_0\rho + \mu)\mathcal{G} + \mu D_0\left(I_1 G_4 + I_2 G_4'\right)][\left(I_1\mathcal{E}_1 G_4 + I_2\mathcal{E}_2 G_4'\right)\mu D_0 + (\alpha_F + \rho_B + \mu)\mathcal{G}]}. \tag{A2.30}$$

From (A2.3),

$$B = \frac{\rho_B F X}{(1-\epsilon_{B1})(\beta_1 I_1 + \beta_2 A_1) + (1-\epsilon_{B2})(\beta_3 I_2 + \beta_4 A_2) + (\alpha_B + \mu)X}.$$

Substituting (A2.23), (A2.25), and (A2.27) gives us

$$B = \frac{\rho_B \mathcal{G}}{\mu D_0[(1-\epsilon_{B1})I_1 G_4 + (1-\epsilon_{B2})I_2 G_4'] + (\alpha_B + \mu)\mathcal{G}} F. \tag{A2.31}$$

From (A2.9), (A2.23), (A2.25), and (A2.27), we get

$$S_p = \frac{(\alpha_B B + \alpha_F F + \eta_1 R_1 + \eta_2 R_2)\mathcal{G}}{\mu D_0[(1-\psi_1)I_1 G_4 + (1-\psi_2)I_2 G_4'] + \mu\mathcal{G}}, \tag{A2.32}$$

Using the expressions for B, F, R_1, and R_2, we can write the above equations in terms of I_1 and I_2. Finally, using (A2.4) and (A2.10), we can obtain a system of two quadratic equations in I_1 and I_2. However, since the resulting equations become too unwieldy, we will analyze them only in the case when the parameter ρ is zero.

A2.2.3. Endemic equilibrium without vaccination

In the case where there is no vaccination except for booster doses, that is, when $\rho = 0$, we obtain the following equations for the endemic equilibrium (the process is analogous to Section A2.2.2):

$$\begin{aligned}
E_1 &= \frac{I_1[\gamma_1(1-\varphi_1) + \sigma\varphi_1 + \mu]}{p_1 w}, \qquad A_1 = \frac{I_1(1-p_1)[\gamma_1(1-\varphi_1) + \sigma\varphi_1 + \mu]}{p_1(\gamma_1 + \mu)}, \\
H_1 &= \frac{\sigma\varphi_1 I_1}{\omega_1 + \mu}, \qquad R_1 = \frac{(G_1 + G_2 + G_3)\, I_1}{p_1(\eta_1 + \mu)D_1}, \\
E_2 &= \frac{I_2[\gamma_2(1-\varphi_2) + \sigma\varphi_2 + \mu]}{p_2 w}, \qquad A_2 = \frac{I_2(1-p_2)[\gamma_2(1-\varphi_2) + \sigma\varphi_2 + \mu]}{p_2(\gamma_2 + \mu)}, \\
H_2 &= \frac{\sigma\varphi_2 I_2}{\omega_2 + \mu}, \qquad R_2 = \frac{\left(G_1' + G_2' + G_3'\right) I_2}{p_2(\eta_2 + \mu)D_1'}, \\
S &= \frac{\Lambda\mathcal{G}}{\mu\mathcal{G} + \mu D_0\left(I_1 G_4 + I_2 G_4'\right)}, \qquad S_p = \frac{(Z_1 I_1 + Z_2 I_2)\mathcal{G}}{\mu D_0[(1-\psi_1)I_1 G_4 + (1-\psi_2)I_2 G_4'] + \mu\mathcal{G}}, \\
F &= 0, \qquad B = 0,
\end{aligned}$$

where

$$Z_1 = \frac{\eta_1\,(G_1 + G_2 + G_3)}{p_1(\eta_1 + \mu)D_1}, \qquad Z_2 = \frac{\eta_2\left(G_1' + G_2' + G_3'\right)}{p_2(\eta_2 + \mu)D_1'}.$$

Furthermore, if $I_1, I_2 > 0$, we can see that the condition $\mathcal{G}(I_1, I_2) > 0$ becomes necessary and sufficient for all other variables to be nonnegative.

Substituting back in equations (A2.4) and (A2.10), we see that I_1 and I_2 satisfy

$$\begin{aligned} P_1 I_1^2 + P_2 I_2^2 + P_3 I_1 I_2 + P_4 I_1 + P_5 I_2 + P_6 = 0, \\ Q_1 I_1^2 + Q_2 I_2^2 + Q_3 I_1 I_2 + Q_4 I_1 + Q_5 I_2 + Q_6 = 0, \end{aligned} \tag{A2.33}$$

where

$$\begin{aligned} P_1 &= (1-\psi_1)(D_0^2 G_4^2 Z_3 + D_0 D_2 G_4 Z_1 \sigma - D_0 D_2 G_4 \sigma Z_3 - D_0^2 G_4^2 Z_1) + D_2^2 \sigma^2 Z_3 - D_0 D_2 G_4 \sigma Z_3, \\ P_2 &= (1-\psi_1)(D_0 D_3 G_4 Z_2 \sigma - D_0^2 G_4 G_4' Z_2) + (1-\psi_2)(D_0^2 G_4'^2 Z_3 - D_0 D_3 G_4' \sigma Z_3) + D_3^2 \sigma^2 Z_3 \\ &\quad - D_0 D_3 G_4' \sigma Z_3, \\ P_3 &= (1-\psi_1)(D_0^2 G_4 G_4' Z_3 + D_0 D_2 G_4 Z_2 \sigma + D_0 D_3 G_4 Z_1 \sigma - D_0 D_3 G_4 \sigma Z_3 - D_0^2 G_4^2 Z_2 - D_0^2 G_4 G_4' Z_1) \\ &\quad + (1-\psi_2)(D_0^2 G_4 G_4' Z_3 - D_0 D_2 G_4' \sigma Z_3) - D_0 D_2 G_4' \sigma Z_3 - D_0 D_3 G_4 \sigma Z_3 + 2 D_2 D_3 \sigma^2 Z_3, \\ P_4 &= (1-\psi_1)(D_0^2 G_4 \Lambda Z_3 - D_0^2 G_4^2 \Lambda - D_0^2 G_4 \Lambda Z_1) + D_0^2 G_4 \Lambda Z_3 + D_0 D_2 G_4 \Lambda \sigma - 2 D_0 D_2 \Lambda \sigma Z_3, \\ P_5 &= (1-\psi_2)(D_0^2 G_4' \Lambda Z_3 - D_0^2 G_4 G_4' \Lambda) - D_0^2 G_4 \Lambda Z_2 (1-\psi_1) + D_0^2 G_4' \Lambda Z_3 + D_0 D_3 G_4 \Lambda \sigma - 2 D_0 D_3 \Lambda \sigma Z_3, \\ P_6 &= D_0^2 \Lambda^2 (Z_3 - G_4), \end{aligned}$$

$$\begin{aligned} Q_1 &= (1-\psi_1)(D_0^2 G_4^2 Z_4 - D_0 D_2 G_4 Z_4 \sigma) + (1-\psi_2)(D_0 D_2 G_4' Z_1 \sigma - D_0^2 G_4 G_4' Z_1) + D_2^2 Z_4 \sigma^2 \\ &\quad - D_0 D_2 G_4 Z_4 \sigma, \\ Q_2 &= (1-\psi_2)(D_0^2 G_4'^2 Z_4 + D_0 D_3 G_4' Z_2 \sigma - D_0 D_3 G_4' Z_4 \sigma - D_0^2 G_4'^2 Z_2) + D_3^2 Z_4 \sigma^2 - D_0 D_3 G_4' Z_4 \sigma, \\ Q_3 &= (1-\psi_1)(D_0^2 G_4 G_4' Z_4 - D_0 D_3 G_4 Z_4 \sigma) + (1-\psi_2)(D_0^2 G_4 G_4' Z_4 + D_0 D_2 G_4' Z_2 \sigma + D_0 D_3 G_4' Z_1 \sigma \\ &\quad - D_0^2 G_4 G_4' Z_2 - D_0^2 G_4'^2 Z_1 - D_0 D_2 G_4' Z_4 \sigma) + 2 D_2 D_3 Z_4 \sigma^2 - D_0 D_2 G_4' Z_4 \sigma - D_0 D_3 G_4 Z_4 \sigma, \\ Q_4 &= (1-\psi_1)(D_0^2 G_4 \Lambda Z_4 - D_0^2 G_4 G_4' \Lambda) - D_0^2 G_4' \Lambda Z_1 (1-\psi_2) + D_0^2 G_4 \Lambda Z_4 + D_0 D_2 G_4' \Lambda \sigma - 2 D_0 D_2 \Lambda Z_4 \sigma, \\ Q_5 &= (1-\psi_2)(D_0^2 G_4' \Lambda Z_4 - D_0^2 G_4'^2 \Lambda - D_0^2 G_4' \Lambda Z_2) + D_0^2 G_4' \Lambda Z_4 + D_0 D_3 G_4' \Lambda \sigma - 2 D_0 D_3 \Lambda Z_4 \sigma, \\ Q_6 &= D_0^2 \Lambda^2 (Z_4 - G_4'), \end{aligned}$$

$$Z_3 = \frac{(w+\mu)[\gamma_1(1-\varphi_1) + \sigma\varphi_1 + \mu]}{p_1 w}, \qquad Z_4 = \frac{(w+\mu)[\gamma_2(1-\varphi_2) + \sigma\varphi_2 + \mu]}{p_2 w}.$$

Therefore, we conclude the following result:

Theorem A2.1. *When $\rho = 0$, system* (A1.1) *has an endemic equilibrium if and only if there exist $I_1, I_2 > 0$ satisfying* (A2.33) *such that*

$$\Lambda D_0 - \sigma(I_1 D_2 + I_2 D_3) > 0.$$

A2.3. Basic reproduction number

The infected compartments of the population are $E_1, I_1, A_1, H_1, E_2, I_2, A_2$, and H_2. Let $m_1 = w + \mu$, $m_2 = \gamma_1(1-\varphi_1) + \sigma\varphi_1 + \mu$, $m_3 = \gamma_1 + \mu$, $m_4 = \omega_1 + \mu$, $m_5 = \gamma_2(1-\varphi_2) + \sigma\varphi_2 + \mu$, $m_6 = \gamma_2 + \mu$, and $m_7 = \omega_2 + \mu$. Using the notation in [39], it follows that the new infections and transition matrices are

given by

$$\mathcal{F} = \begin{pmatrix} \left(\frac{\beta_1 I_1 + \beta_2 A_1}{X}\right)[S + (1-\psi_1)S_p + \mathcal{E}_1 F + (1-\epsilon_{B1})B] \\ 0 \\ 0 \\ 0 \\ \left(\frac{\beta_3 I_2 + \beta_4 A_2}{X}\right)[S + (1-\psi_2)S_p + \mathcal{E}_2 F + (1-\epsilon_{B2})B] \\ 0 \\ 0 \\ 0 \end{pmatrix},$$

$$\mathcal{V} = \begin{pmatrix} m_1 E_1 \\ -p_1 w E_1 + m_2 I_1 \\ -(1-p_1) w E_1 + m_3 A_1 \\ -\sigma\varphi_1 I_1 + m_4 H_1 \\ m_1 E_2 \\ -p_2 w E_2 + m_5 I_2 \\ -(1-p_2) w E_2 + m_6 A_2 \\ -\sigma\varphi_2 I_2 + m_7 H_2 \end{pmatrix}.$$

Then,

$$F = \begin{pmatrix} 0 & \mathcal{M}_1 & \mathcal{M}_2 & 0 & 0 & 0 & 0 & 0 \\ 0 & 0 & 0 & 0 & 0 & 0 & 0 & 0 \\ 0 & 0 & 0 & 0 & 0 & 0 & 0 & 0 \\ 0 & 0 & 0 & 0 & 0 & \mathcal{M}_3 & \mathcal{M}_4 & 0 \\ 0 & 0 & 0 & 0 & 0 & 0 & 0 & 0 \\ 0 & 0 & 0 & 0 & 0 & 0 & 0 & 0 \\ 0 & 0 & 0 & 0 & 0 & 0 & 0 & 0 \end{pmatrix},$$

$$V = \begin{pmatrix} m_1 & 0 & 0 & 0 & 0 & 0 & 0 & 0 \\ -p_1 w & m_2 & 0 & 0 & 0 & 0 & 0 & 0 \\ -(1-p_1)w & 0 & m_3 & 0 & 0 & 0 & 0 & 0 \\ 0 & -\sigma\varphi_1 & 0 & m_4 & 0 & 0 & 0 & 0 \\ 0 & 0 & 0 & 0 & m_1 & 0 & 0 & 0 \\ 0 & 0 & 0 & 0 & -p_2 w & m_5 & 0 & 0 \\ 0 & 0 & 0 & 0 & -(1-p_2)w & 0 & m_6 & 0 \\ 0 & 0 & 0 & 0 & 0 & -\sigma\varphi_2 & 0 & m_7 \end{pmatrix},$$

where

$$\mathcal{M}_1 = \frac{\beta_1\left[S^0 + \mathcal{E}_1 F^0 + (1-\epsilon_{B1})B^0 + (1-\psi_1)S_p^0\right]}{S^0 + F^0 + B^0 + S_p^0}, \quad \mathcal{M}_2 = \frac{\beta_2\left[S^0 + \mathcal{E}_1 F^0 + (1-\epsilon_{B1})B^0 + (1-\psi_1)S_p^0\right]}{S^0 + F^0 + B^0 + S_p^0},$$

$$\mathcal{M}_3 = \frac{\beta_3\left[S^0 + \mathcal{E}_2 F^0 + (1-\epsilon_{B2})B^0 + (1-\psi_2)S_p^0\right]}{S^0 + F^0 + B^0 + S_p^0}, \quad \mathcal{M}_4 = \frac{\beta_4\left[S_0 + \mathcal{E}_2 F^0 + (1-\epsilon_{B2})B^0 + (1-\psi_2)S_p^0\right]}{S^0 + F^0 + B^0 + S_p^0}.$$

Calculating the inverse of V, we get

$$V^{-1} = \begin{pmatrix} \frac{1}{m_1} & 0 & 0 & 0 & 0 & 0 & 0 & 0 \\ \frac{p_1 w}{m_1 m_2} & \frac{1}{m_2} & 0 & 0 & 0 & 0 & 0 & 0 \\ \frac{(1-p_1)w}{m_1 m_3} & 0 & \frac{1}{m_3} & 0 & 0 & 0 & 0 & 0 \\ \frac{\sigma p_1 w \varphi_1}{m_1 m_2 m_4} & \frac{\sigma \varphi_1}{m_2 m_4} & 0 & \frac{1}{m_4} & 0 & 0 & 0 & 0 \\ 0 & 0 & 0 & 0 & \frac{1}{m_1} & 0 & 0 & 0 \\ 0 & 0 & 0 & 0 & \frac{p_2 w}{m_1 m_5} & \frac{1}{m_5} & 0 & 0 \\ 0 & 0 & 0 & 0 & \frac{(1-p_2)w}{m_1 m_6} & 0 & \frac{1}{m_6} & 0 \\ 0 & 0 & 0 & 0 & \frac{\sigma p_2 w \varphi_2}{m_1 m_5 m_7} & \frac{\sigma \varphi_2}{m_5 m_7} & 0 & \frac{1}{m_7} \end{pmatrix}.$$

Multiplying F and V^{-1}, we get

$$FV^{-1} = \begin{pmatrix} \frac{\mathcal{M}_1 w p_1 m_3 + \mathcal{M}_2 w (1-p_1) m_2}{m_1 m_2 m_3} & \frac{\mathcal{M}_1}{m_2} & \frac{\mathcal{M}_2}{m_3} & 0 & 0 & 0 & 0 & 0 \\ 0 & 0 & 0 & 0 & 0 & 0 & 0 & 0 \\ 0 & 0 & 0 & 0 & 0 & 0 & 0 & 0 \\ 0 & 0 & 0 & 0 & 0 & 0 & 0 & 0 \\ 0 & 0 & 0 & 0 & \frac{\mathcal{M}_3 w p_2 m_6 + (1-p_2) w m_5 \mathcal{M}_4}{m_1 m_5 m_6} & \frac{\mathcal{M}_3}{m_5} & \frac{\mathcal{M}_4}{m_6} & 0 \\ 0 & 0 & 0 & 0 & 0 & 0 & 0 & 0 \\ 0 & 0 & 0 & 0 & 0 & 0 & 0 & 0 \\ 0 & 0 & 0 & 0 & 0 & 0 & 0 & 0 \end{pmatrix},$$

which has the eigenvalues $\lambda_1 = \frac{\mathcal{M}_1 w p_1 m_3 + \mathcal{M}_2 w (1-p_1) m_2}{m_1 m_2 m_3} > 0$, $\lambda_2 = \frac{\mathcal{M}_3 w p_2 m_6 + \mathcal{M}_4 (1-p_2) w m_5}{m_1 m_5 m_6} > 0$, and $\lambda_i = 0$, $i \in \{3, 4, 5, 6, 7, 8\}$.

Therefore, the basic reproduction number with vaccination, also known as the control reproduction number, is given by

$$\mathcal{R}_c = \max\{\mathcal{R}_a, \mathcal{R}_b\},$$

where

$$\mathcal{R}_a = \frac{w\mathcal{M}_1 p_1 m_3 + w\mathcal{M}_2 (1-p_1) m_2}{m_1 m_2 m_3} = \frac{w\mathcal{M}_1 p_1 (\gamma_1 + \mu) + w\mathcal{M}_2 (1-p_1)[\gamma_1 (1-\varphi_1) + \sigma\varphi_1 + \mu]}{(w+\mu)[\gamma_1 (1-\varphi_1) + \sigma\varphi_1 + \mu](\gamma_1 + \mu)},$$

$$\mathcal{R}_b = \frac{w\mathcal{M}_3 p_2 (\gamma_2 + \mu) + w\mathcal{M}_4 (1-p_2) m_5}{m_1 m_5 m_6} = \frac{w\mathcal{M}_3 p_2 (\gamma_2 + \mu) + w\mathcal{M}_4 (1-p_2)[\gamma_2 (1-\varphi_2) + \sigma\varphi_2 + \mu]}{(w+\mu)[\gamma_2 (1-\varphi_2) + \sigma\varphi_2 + \mu](\gamma_2 + \mu)}.$$

In the particular case when $\rho = 0$, we can obtain the basic reproduction number with no vaccination, $\mathcal{R}_0$, which is given by the expression

$$\mathcal{R}_0 = \max\left\{\frac{w\beta_1 p_1(\gamma_1+\mu) + w\beta_2(1-p_1)[\gamma_1(1-\varphi_1)+\sigma\varphi_1+\mu]}{(w+\mu)[\gamma_1(1-\varphi_1)+\sigma\varphi_1+\mu](\gamma_1+\mu)}, \right.$$
$$\left.\frac{w\beta_3 p_2(\gamma_2+\mu) + w\beta_4(1-p_2)[\gamma_2(1-\varphi_2)+\sigma\varphi_2+\mu]}{(w+\mu)[\gamma_2(1-\varphi_2)+\sigma\varphi_2+\mu](\gamma_2+\mu)}\right\}.$$

Furthermore, by [39, Theorem 2], we can conclude the following result, which ensures the threshold dynamics of the disease-free equilibrium.

Theorem A2.2. *The disease-free equilibrium E_0 of system* (A1.1) *is locally asymptotically stable if $\mathcal{R}_c < 1$ and unstable if $\mathcal{R}_c > 1$.*

AIMS Press